Particuology 116 (2026) 448–466

Contents lists available at ScienceDirect

Particuology

journal homepage: www.elsevier.com/locate/partic

Recycled Arabic gum as a replacement for starch in self-reducing mill scale-based briquettes

Sara Scolari*, Luca Tosarello, Davide Mombelli, Gianluca Dall'Osto, Carlo Mapelli

Politecnico di Milano, Dipartimento di Meccanica, Via Privata Giuseppe La Masa 1, 20156, Milano, Italy

HIGHLIGHTS

- Arabic gum increases the IRI and thermal stability of each mixture.
- Viscosity of the binder affects particles orientation during briquetting.
- No alteration of chemical composition and microstructure after reduction.
- Arabic gum can cover up to 46% of briquettes production.

GRAPHICAL ABSTRACT

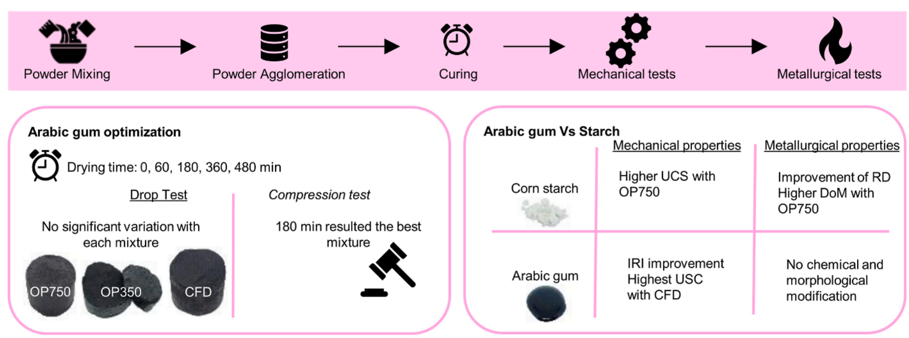

ARTICLE INFO

Keywords:
Self-reducing briquettes
Arabic gum
Starch
Mechanical properties
Metallurgical properties

ABSTRACT

Steelmaking produces large quantities of iron-rich by-products and their recycling improves resource efficiency and reduces waste generation. This work investigates the potential for utilizing mill scale to produce self-reducing briquettes assessing the effectiveness of recycled Arabic gum as a sustainable binder compared to conventional starch. The briquettes were produced by combining the mill scale with different reducing agents: olive pomace biochar pyrolyzed at 750 (OP750) and 350 °C (OP350), and cupola furnace dust (CFD). By using Arabic gum instead of starch, an improved resistance to impact was observed for each mixture (1000 for OP750 and CFD versus 767 and 191, respectively). Recycled Arabic gum, also, limited the swelling of each mixture and promoted the sintering of the briquettes. On the contrary, the starch favored an increase in volume (maximum 153.62%) until 1200 °C. Furthermore, the Arabic gum enhanced the reduction capacity of the mixture while preventing chemical or morphological variations in the reduction products and leading to an increase of up to 9.06% in the degree of metallization with OP350. Overall, most the results obtained using Recycled Arabic gum exceeded the industrial benchmark, confirming the feasibility of its usage as a substitute for starch in self-reducing briquettes.

* Corresponding author.
E-mail address: sara.scolari@polimi.it (S. Scolari).

https://doi.org/10.1016/j.partic.2026.06.039
Received 9 April 2026; Received in revised form 29 June 2026; Accepted 30 June 2026
Available online 11 July 2026

1. Introduction

In recent years, the valorization of steelmaking by-products, such as dust and sludge, through agglomeration processes has emerged as a promising strategy to combine resource recovery with the reduction of the environmental impact of metallurgical processes (Abdelrahim et al., 2021; Echterhof et al., 2019; Mantovani et al., 2002; Mombelli et al., 2016, 2019; Mombelli et al., 2021; Nath et al., 2017; Scolari et al., 2026; Scolari, Mombelli, et al., 2025; Takano & Mourao, 2003; Trpčevská et al., n.d.; Yu et al., 2014). In particular, the production of self-reducing agglomerates (e.g., briquettes, pellets) based on iron-bearing residues and carbonaceous reductants has been widely investigated as a route to recycle steelmaking wastes. Despite the large number of studies in the literature proving the feasibility of using carbothermal reduction to recover strategic metals from such waste, the agglomerates do not always meet the mechanical requirements necessary for industrial application.

One of the key factors affecting the performance of self-reducing agglomerates is the nature of the binder, its amount used, its compatibility and its interaction with the matrices utilized. Several organic binders have been indeed investigated for metallurgical agglomeration, including starch, molasses, bitumen, carboxymethyl cellulose (CMC), and biomass-derived materials (Abdelrahim et al., 2022; Mousa et al., 2022). Starch is widely used in literature, in particular by the same authors (Dall'Osto, Mombelli, Trombetta, & Mapelli, 2024; Dall'Osto et al., 2024; Drobíková et al., 2016; Lohmeier et al., 2020; Mombelli et al., 2021; Scolari et al., 2026; Scolari, Mombelli, et al., 2025). It is mostly preferred over inorganic binders, such as bentonite, thanks to the lower environmental impact and lower acidic species content (e.g., SiO_2). However, in several cases, in which powders and fines are agglomerated in the form of briquettes, they exhibit insufficient resistance to drop or compression tests, thus limiting their practical applicability and highlighting the need for improvements in formulation and processing parameters. For instance, briquettes made in red mud required a superior amount of water mixed with starch before the gelatinization to guarantee self-standing ability (Scolari, Dall'Osto, et al., 2025); briquettes rich of belt conveyor fines and bounded with starch broke after only a few drops (Abdelrahim et al., 2021) and the ultimate compression strength of briquettes made of ferromanganese and charcoal fines ranged only between 1.63 and 7.04 MPa according to the optimization process and binder used (bentonite, molasses and starch) (De Melo Silva Cheloni et al., 2024). Typically, the minimum cold compression strength requirement is 9.8 MPa for metallurgical applications inside a converter (Barisetty et al., 2020; Mousa et al., 2022) also showed that bitumen was the only tested organic binder which avoids the deterioration of the mechanical strength of the briquettes and enhances the reduction rate.

In the context of utilizing alternative organic binders to starch, Arabic gum has received limited attention in metallurgical agglomeration despite its strong adhesive properties and potential contribution of additional carbon into biomass briquettes (Okegbile et al., 2014; Yahaya & Ibrahim, 2012). However, it has shown promising results in the agglomeration of magnetite iron ore (Koohestani et al., 2025). This study represents the first reported use of Arabic gum as a binder in a metallurgical application, highlighting its potential for integration into ironmaking and steelmaking processes. Subsequently (Scolari et al., 2026), demonstrated that substituting starch with Arabic gum significantly improved the mechanical behavior of self-reducing briquettes produced by mixing dust from a basic oxygen furnace (BOF) and blast furnace sludge (BFS). This resulted in an improvement in the impact resistance index from 125 to 1000, as well as preventing the breakage of briquettes during thermal treatment. The use of Arabic gum therefore enabled the limitations observed with starch to be overcome while maintaining the advantages associated with organic binders. However, this positive effect could not be transferred to all material combinations due to interactions between the binder, the iron-bearing matrix and the reductant affecting the final properties of the agglomerates. For instance, the impact resistance index of agglomerates made of coarse particle (>125 μm) was reduced from 1000 to 188 using Arabic gum (Scolari et al., 2026). For this reason, additional studies involving different matrices are required in order to clarify under which conditions Arabic gum can effectively improve briquette performance.

Although Arabic gum has demonstrated promising binding performances in several agglomeration processes, its widespread industrial application is often limited by its relatively high cost (7.62 \$ kg^{-1} (tridge.,)"https://www.tridge.com; Last Access 01/09/2025" n.d.) and restricted geographical availability (bayrony,) ("https://bayrony.com/product-enquiry/products/gum-arabic/" n. d.). To overcome these limitations within a circular economy framework, alternative sources of Arabic gum can be considered. In particular, Arabic gum is extensively used in the wine industry as a stabilizing agent to improve colloidal stability and prevent precipitation phenomena (Apolinar-Valiente et al., 2020a; Nigen et al., 2019a; Sanchez et al., 2018). This application generates waste streams containing residual Arabic gum that are currently underutilized. The recovery and reuse of these secondary streams as binders for the agglomeration of steelmaking by-products could represent a valuable industrial symbiosis approach, simultaneously reducing waste generation in the food sector and decreasing the consumption of natural binding materials in the metallurgical industry (Scolari et al., 2026). indeed already demonstrated the possibility to substitute the natural Arabic gum with a recycled solution coming from the wine industry without affecting the mechanical and metallurgical properties of the agglomerate.

Traditionally, the reducing agents for iron oxides had fossil origin, such as semi-coke, coke powder or anthracite (Ning et al., 2025). However, the growing pressure from global energy demand and the persistent dependence on fossil fuels have determined a significant increase in greenhouse gas emissions, making the identification of alternative and sustainable solutions increasingly urgent (Chen et al., 2015). In this regard, olive pomace is of particular interest due to its high energy content and huge seasonal availability in the Mediterranean region. The latter accounts for over 98% of the global olive oil production (approx. 2.5 million ton per year), with Spain, Italy, Greece and Portugal as leading producers (Valenti et al., 2017). It is a solid residue obtained following the crushing and pressing operations of olives for oil extraction. After a possible recovery of residual oil, it is generally dried and destined for disposal or sold to other companies for further extraction process (Kabakcı & Aydemir, 2014). From a circular economy perspective, one of the most promising and largely studied (Lustosa Filho et al., 2024) valorization strategies is the conversion of pomace through pyrolysis processes to obtain bio-oil, gas and a solid carbonaceous residue known as biochar (Raveendran & Ganesh, 1996).

An interesting case study is represented by the work of Dall'Osto et al. (2024), who investigated the behavior of self-reducing briquettes made by mill scale and biogenic carbons bounded with starch. Mill scale is a by-product generated continuously during hot rolling and forging operations, typically in amounts of approximately 2 wt% of the steel produced ((eurofer.,) "https://www.eurofer.eu/publications/brochures-booklets-and-factsheets/european-steel-in-figures-2025, access on 18-02-2026" n. d.; (ispatguru.,)"https://www.ispatguru.com/mill-scale/, access on 20-03-26" n. d.). It is characterized by a content of iron oxides higher than 70 wt% (Ilutiu-Varvara et al., 2020), and, compared to other steel residues such as dust and sludge, it generally has a relatively 'clean' composition and is free of critical contaminants, such as Zn, Pb or alkalis (Ilutiu-Varvara et al., 2020; Quddus et al., 2018). This makes it an ideal iron carrier for studying and developing self-reducing agglomerates, as its pure composition minimizes material heterogeneity and enables the effects of different parameters, such as the reducing agent or binder, to be clearly identified and assessed (Bagatini et al., 2020; Dall'Osto et al., 2024; Elsadek et al., 2024; Kumar et al., 2017).

The results obtained by Dall'Osto et al. (2024) showed that the physicochemical properties of the reductant significantly affected both the cold mechanical response (impact resistance and compression strength) and the metallurgical behavior at high temperatures (degree of reduction and degree of metallization). However, not all the briquettes guaranteed mechanical and metallurgical performance compatible with the industrial requirements. Neither mixture survived to 10 drops, and the briquettes made of olive pomace pyrolyzed at 350 °C exhibited an ultimate compression strength that was 50% lower than the required value for blast furnaces or shaft furnaces (Richards, 1990). These limitations make this system particularly suitable as a reference case to investigate possible improvements in briquette formulation.

Based on these considerations, this work aims to evaluate whether the substitution of starch with recycled Arabic gum can improve the performance of self-reducing briquettes produced from mill scale-based mixtures. The same formulations previously investigated by Dall'Osto et al. (2024) are considered, consisting of mill scale combined with two types of pyrolyzed olive pomace at 350 and 750 °C. This allows a direct comparison between the two binders and an assessment of the effect of replacing starch with recycled Arabic gum on the mechanical properties and metallurgical behavior of the briquettes.

This work is intended as a proof of concept to verify whether the positive effects of recycled Arabic gum observed in previous studies (Scolari et al., 2026) can be extended to different materials. Demonstrating a similar improvement in briquettes based on mill scale and biogenic carbons would lend support to the hypothesis that recycled Arabic gum could be a versatile alternative binder for self-reducing agglomerates. At the same time, this study expands the range of material combinations in which this binder has been evaluated and helps clarify the conditions under which its use is advantageous. To further strengthen this assessment, the same comparative approach is also applied to mixtures in which the reducing agent is a dust collected from a cupola furnace.

2. Materials and methods

2.1. Materials characterization

The briquettes were produced mixing the mill scale (MS) as iron carrier and three reducing agents: olive pomace pyrolyzed at 750 °C (OP750), olive pomace pyrolyzed at 350 °C (OP350), and cupola furnace dust (CFD). The chemical composition of the MS and CFD, obtained by means of wavelength-dispersive X-ray fluorescence (WD-XRF) with a Bruker S8 Tiger spectrometer (Bruker, Billerica, Massachusetts, US), is reported in Table 1. The total carbon was obtained by using the combustion analyzer Bruker G4 ICARUS (Bruker, Billerica, Massachusetts, US).

The four matrices were mineralogically characterized through X-ray diffraction (XRD) by Rigaku SmartLab SE diffractometer (Rigaku Corporation, Tokyo, Japan) in θ-θ configuration (Cu-Kα radiation: $\lambda = 1.54$ Å at 40 kV, 40 mA). The analysis was accomplished with a scan range of 5−90° 2θ through a 1D/teX Ultra 250 detector featured by XRF suppression filter; the powdered materials were scanned at 2° min^{-1} with a step size of 0.02° and rotated at 60 rpm. The quantitative analysis of the MS phases was performed by Rietveld method. The XRD pattern of CFD is shown in Fig. 1.

MS, OP350 and OP750 were already characterized by (Dall'Osto et al., 2023; 2025), hence their XRD patterns are not reported. The summary of the proximate analysis results and total carbon of the biochar used is shown in Table 2. Specifically, the amount of volatile matter (VM), fixed carbon (FC) and ash were evaluated by means of thermogravimetric and differential scanning calorimetry (TG-DSC) according to the ASTM D1762-84 standard using a Netzsch STA 449 F^3 Jupiter (Erich NETZSCH B.V. & Co. Holding KG, Selb, Germany). Whereas, total carbon was calculated by means of a LECO CS230 elemental analyzer (LECO Corporation, St. Joseph, Michigan, USA).

The granulometric distribution was determined using an optical granulometer (Malvern Morphology 4, Malvern, UK) equipped with 25X, 100X and 200X lens. For each sample analyzed, cumulative volume distribution curves were obtained and the D10, D50, and D90 percentiles were calculated. The main statistical parameters obtained are reported in Table 3, including also the volume mean diameter D4,3, as well as the surface mean diameter D3,2 ((horiba.,) "https://www.horiba.com/int/scientific/products/particle-characterization/particle-education/setting-particle-size-specifications/" n. d.). The analysis was not performed on MS due to its scale-shape and morphology, which would have required mechanical grinding and thereby altered the true particle size distribution. However, a granulometric distribution obtained from the weight fraction of mill scale which passes different sieve openings (from 2 mm to 63 μm) was reported by Dall'Osto et al. (2026).

The water-powder interaction of the reducing agents was detected through sessile drop test according to BS EN ISO 19403 after the compaction through a mechanical press of few grams of powder inside a compact disk according to ASTM D7334 - 08 (2017). OP350 and CFD were hydrophobic with contact angle of 146.98° and 117.41°, respectively. OP750 was instead hydrophilic with a contact angle of 52.02°.

2.2. Briquettes preparation

To maintain continuity with the previous work of Dall'Osto et al. (2024), the sieved fraction of MS lower than 125 μm and of reducing agents lower than 63 μm, were considered. The powders were then agglomerated in pairs. MS and reducing agents were balanced to tailor the amount of carbon to the iron oxides inside each mixture, thereby ensuring the latter's complete reduction. The resulting ratios were 3.6:1 for MS_OP750, 3.4:1 for MS_OP350 and 2:1 for MS_CFD. One binder type was then added to each powder mixture. Corn starch (_CS) was dosed to reach 5 wt% of the total dry powders, it was then mixed with distilled water (a water-starch ratio of 6:1 by mass) and subsequently heated for 30 min at 100 °C to get retrogradation up to 30% (Dall'Osto, Mombelli, Trombetta, & Mapelli, 2024). Important to notice is that the mixtures MS_OP350_CS and MS_OP750_CS were already characterized by Dall'Osto et al. (2024), and their results are therefore considered to be reliable. The second batch used an aqueous solution of recycled Arabic gum (_AG) supplied by AEB S. p.A. In order to understand how to dose the recycled Arabic gum to reach sufficient mechanical results, a preliminary experimental campaign was performed. The raw solution was subjected to drying treatment for different times (10, 30, 60, 120, 180, 240, 360 and 480 min), using Carbolite HRF 722 D furnace (Carbolite Gero Ltd., Hope Valley, UK) at the constant temperature of 105 °C. It was stirred every 30 min, to reduce the amount of water, and consequently increase the solid fraction inside the binder. To ensure a consistent comparison with starch, the recycled Arabic gum solution was added in an amount such that the dry Arabic gum content contributed exactly 5 wt% of the total dry powder mass. Consequently, the dosage was based on binder solids rather than on the total mass of the aqueous solution. This approach also enables a parallel assessment of how variations in water content influence the results while keeping a key binder-related parameter, namely the amount of active binder solids, constant.

Briquettes of 20 mm in diameter and 20 mm in height were produced

Table 1
Chemical composition of mill scale and cupola furnace dust expressed in wt.%. ("-" means not detected).

Sample	Fe_2O_3	Fe_3O_4	FeO	FeOx	SiO_2	Al_2O_3	CaO	MgO	MnO	Cr_2O_3	CuO	NiO	Ctot
MS	46.30	19.40	34.30	96.95	0.60	0.30	0.32	0.07	0.30	0.32	0.07	0.08	-
CFD	-	-	-	26.35	8.48	3.30	3.31	0.89	0.16	-	-	-	44.11

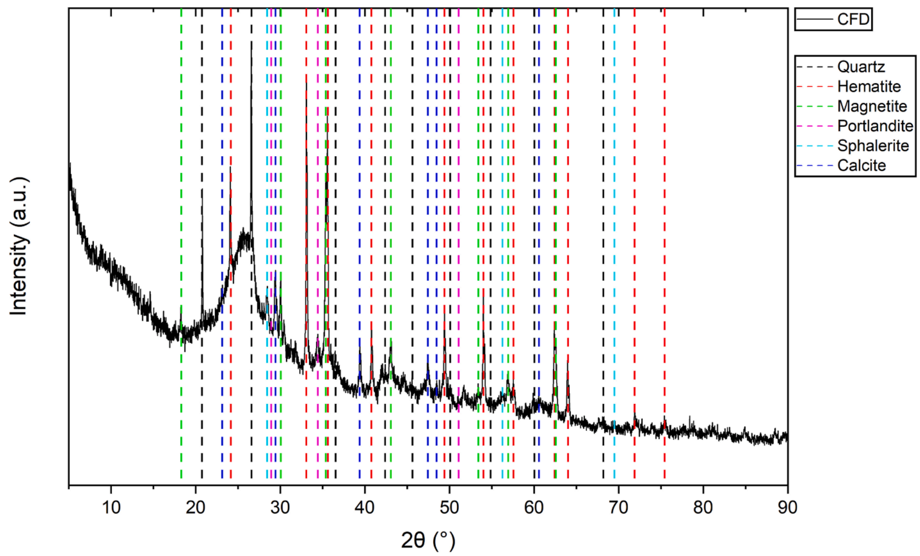

Fig. 1. XRD patter of cupola furnace dust (quartz SiO_2, hematite Fe_2O_3, magnetite Fe_3O_4, portlandite $Ca(OH)_2$, sphalerite FeS, calcite $CaCO_3$).

Table 2
Proximate analysis of biochar expressed in wt.% (* refers to the dry base material).

Sample	Volatile Matter*	Fixed Carbon*	Ash*	Total Carbon
OP350	62.55	21.22	16.22	65.23
OP750	51.90	31.14	16.96	69.87

Table 3
Particle size distribution of the reducing agents expressed in μm (D10, D50 and D90 are the diameter percentiles, D4,3 the volume mean diameter and D3,2 the surface mean diameter).

Sample	D10	D50	D90	D4,3	D3,2
OP750	42.74	183.75	513.74	250.27	102.45
OP350	76.02	138.19	405.51	172.58	110.54
CFD	35.46	111.67	358.33	143.94	71.28

using a modified MTS Exceed Series 40 (MTS Systems, Eden Prairie, MN, USA) uniaxial tensile test machine. A constant speed of 20 mm min^{-1} was applied until the pressure reached 40 MPa and then maintained for about 2 min.

After a mechanical characterization of the briquettes produced, the best drying time was selected to agglomerate all the mixtures. The choice of the best drying time was supported by Bonferroni statistical analysis. The level of significance (α) was set at 5%.

Pre- and post-reduced briquettes were then analyzed through a Zeiss Sigma 500 Field Emission Gun Scanning Electron Microscope (FEG-SEM) equipped with an Oxford Xmax Ultim 65 Energy-Dispersive X-Ray Spectroscopy (EDS) probe and Unity BeX (Oxford INCA, Oxford Instruments, High Wycombe, UK).

The porosity of the cured briquettes was calculated according to (Ezeakacha et al., 2018; Rabbani & Salehi, 2017) using Matlab (R2022b, update 10) software. The darker spaces inside the SEM images detected using Otsu multi-level thresholding over gray-scale were considered as porous and they were measured using the algorithm Watershed. It should be noted that this image-based approach provides a two-dimensional estimation of porosity and therefore should be considered as a comparative rather than an absolute measurement of the total three-dimensional pore volume.

Only the briquettes bounded with Arabic gum and MS_CFD_CS were characterized according to the following conditions. Since the previous work was followed as reference, refer to (Dall'Osto et al., 2024) for the detailed characterization of biochar starch-bounded briquettes.

2.3. Mechanical characterization

The impact resistance of briquettes after curing was evaluated by means of drop test, based on the ASTM D440–07 (2019). Each sample was manually released from a height of 1.63 m onto a steel container of nearly 1 m^2, large enough to prevent material loss. A 100 mm U-shaped steel semi-tube was used to ensure both vertical alignment and test repeatability. Due to the absence of a specific standard for steelmaking agglomerates, the test was repeated for 3 briquettes of each mixture to obtain a statistical analysis. The test was stopped either after 10 drops or earlier if a detached fragment exceeded 5 wt% of the briquette's initial mass. The size stability factor (s) of the briquettes was calculated with Eq. (1).

$$s = \sum_i \% \; wt_i \cdot NF_i \tag{1}$$

where wt_i is the weight of the *i-sm* fraction collected in each sieve with opening size of 6.7, 5.6, 4.0, 2.0, 1.0, 0.5 and 0.125 mm. NF_i is expressed as Eq. (2).

$$NF_i = \frac{(Opening_i + Opening_{i+1})/2}{(Opening_{max} + Opening_{max+1})/2} \tag{2}$$

The Impact Resistance Index (IRI) was calculated with Eq. (3) (Blesa et al., 2003). The average number of pieces was obtained by counting the number of fragments that weighed 5% or more than the initial mass of the briquette (Adu-Poku et al., 2022).

$$IRI = 100 \times \frac{Average\ number\ of\ drops}{Average\ number\ of\ pieces} \tag{3}$$

The Adjusted Impact Resistance Index (AIRI), calculated with Eq. (4), considered the powder detached during the drop test and required the calculation of the Adjusting Factor according to Eq. (5). The latter was obtained from the Adjusting Mass Factor calculated with Eq. (6) considering the mass retained in each sieve with an opening size smaller than 4.0 mm and the final mass collected at the end of the test.

$$AIRI = IRI \cdot Adjusting\ Factor \tag{4}$$

$$Adjusting\ Factor = 1 - \frac{Adjusting\ Mass\ Factor}{Final\ mass} \tag{5}$$

$$Adjusting\ Mass\ Factor = \sum_i \frac{4}{S_i} \cdot M_i \tag{6}$$

where M_i is the mass retained by the *i-sm* sieve and S_i is the sieve opening passed. Lower AIRI corresponds to the detachment of finer particles. If the Adjusting Factor is negative, it should be considered as zero.

If the briquette survived to 10 falls, it was then compressed according to BS ISO 4700:2015, to evaluate the ultimate compressive strength (UCS) (the biochar-starch-based briquettes were instead compressed without performing a prior drop test (Dall'Osto et al., 2024). The sample was pre-loaded between two flat plates at 30 N and pressed at a constant speed of 15 mm min^{-1} until the load falls by 50% of UCS or when the gap between the plates was reduced by more than 50% of the briquette diameter (10 mm).

2.4. Metallurgical characterization

Briquettes were thermally treated at 750, 900, 1050 and 1200 °C inside a Nabertherm LBT 02/17 lift-bottom furnace (Nabertherm GmbH, Lilienthal, Germany) using an inert atmosphere (Ar) by imposing a heating ramp of 100 °C min^{-1} and the maintenance time of 15 min at the desired temperature.

The reduction degree (RD) was calculated with Eq. (7).

$$RD = \frac{m_{wet} - m_{HT}}{m_c + m_O + m_{binder} + m_{volatile}} \times 100 \tag{7}$$

where m_{wet} is the mass of the green briquette, m_{HT} is the mass of the reduced briquette. The theoretical maximum loss of mass achieved by the mixture completely reduced at 1500 °C has been evaluated starting from the initial chemical composition of the briquettes and considering the masses of volatile compounds such as Zn, Cl and alkalis as $m_{volatile}$, the oxygen (m_o) released during the reduction, carbon mass (m_c) consumed and the binder (m_{binder}) which completely volatilizes during the heating.

Swelling index was calculated according to BS ISO 4698:2022 with Eq. (8) considering the apparent volume and neglecting the internal porosities of agglomerates.

$$Swelling = \frac{\Delta V}{V_i} \times 100 \tag{8}$$

where ΔV is the difference between the volume of the briquette after the thermal treatment and its initial volume V_i. Due to the conservation of the briquette's shape after the thermal treatment when agglomerated with recycled Arabic gum, the initial and final volumes were calculated assuming the briquette as a perfect cylinder.

A fifth thermal treatment at 1400 °C under the same inert atmosphere was performed to evaluate the feasibility of smelting the reduced iron and to investigate its resulting microstructure. The degree of metallization (DoM) at 1400 °C (Eq. (9)) was determined through quantitative metallography (Leino et al., 2020). The analysis was performed by post-processing five backscattered electron (BSE) micrographs acquired randomly along the polished surface of each sample with magnification of 300X.

$$DoM\ [\%] = \frac{n_{Fe} \cdot \rho_{Fe}}{n_{Fe} \cdot \rho_{Fe} + n_{FeOx} \cdot \rho_{FeOx} \cdot \chi} \times 100 \tag{9}$$

where n_{Fe} is the number of pixels attributed to metallic iron, ρ_{Fe} is the density of metallic iron, n_{FeO} is the number of pixels corresponding to iron oxides, ρ_{FeOx} is the density of iron oxides, and χ is the weight percentage of iron in the specific oxide phase identified.

3. Results and discussion

3.1. Preliminary experimental campaign

Fig. 2 shows the variation of solid fraction inside the recycled Arabic gum as function of the drying time during the thermal treatment at 105 °C.

No significant changes in mass happened for times less than 60 min, obtaining residual moisture similar to those of undried Arabic gum (73.50 wt%). The contradictory result compared to the experimental campaign lead by Scolari et al. (2026) relied on the experimental procedure. In the previous work, the binder was mixed with the powders before the drying treatment and in 60 min the moisture was reduced to 35 wt%. In this case, however, the powders were mixed only after recycled Arabic gum drying. The management of a higher amount of liquid resulted in longer treatment time to achieve comparable moisture loss. However, this can be considered an advantage for the industrial applicability of the recycled Arabic gum since it demonstrated that the binder could be stock in the already dried form, thereby avoiding the drying procedure of each batch.

As the amount of water in the binder solution has a significant impact on the mechanical properties of the resulting agglomerates (Scolari, Dall'Osto, et al., 2025; Scolari, Mombelli, et al., 2025), only drying conditions involving a moisture content variation of more than 5 wt% were considered. Therefore, the undried recycled Arabic gum (moisture 73.50 wt%), drying time of 60 min (moisture 70.82 wt%), 180 min (moisture 65.31 wt%), 360 min (moisture 56.21 wt%) and 480 min (moisture 44.47 wt%) were selected.

Fig. 3 shows the green and cured density of each briquette bonded with the recycled Arabic gum as function of its moisture content.

Decreasing the amount of water in the recycled Arabic gum mixed in MS_OP750, the green density of the briquettes decreased accordingly. However, the cured density stabilized around 2.20 g cm^{-3} independently from the moisture content. Therefore, irrespectively of initial water-solid ratio of the recycled Arabic gum all the excess of water present in this latter was expelled. In other words, the briquettes absorbed only the amount of water required to reach an adequate level of densification and to ensure sufficient self-standing ability after forming. Any additional water introduced with the recycled Arabic gum was not effectively incorporated into the briquette structure; instead, once the solid particles had absorbed the moisture necessary for packing and binder distribution, the excess water was progressively expelled from the system during the curing stage.

Briquettes made of MS_OP350 and MS_CFD showed similar curing behavior, stabilizing at 1.79 and 2.56 g cm^{-3}, respectively. However, an unexpected behavior was observed during the curing of the MS_OP350 and MS_CFD briquettes bounded with undried recycled Arabic gum. This peculiar behavior was associated to the hydrophobic nature of OP350 and CFD, which limited the absorption of the large quantity of water present in the mixture (Sachdev et al., 2025). Specifically, rather than being absorbed by the powder, the excess water was expelled during compaction and accumulated in the upper part of the mold. This assumption was also confirmed by the compaction curves of such briquettes. As shown in Fig. 4(b) and (c), the MS_OP350 and MS_CFD briquettes containing undried recycled Arabic gum reached the maximum pressure approximately 10 s earlier than the other mixtures. As a consequence, an incompressible water layer was formed, which facilitated the earlier attainment of the pressure peak compared to the dried variants, resulting in a less effective agglomeration process (Fine & Millero, 1973). This phenomenon was instead not observed for mixtures made of OP750. Due to its hydrophilic nature, OP750 absorbed a larger amount of water, preventing the formation of the incompressible liquid layer. As a consequence, the loading history remained essentially unchanged regardless of the drying time (Fig. 4a), leading to similar particle packing and final densification.

The observation of the agglomeration curves also provided some

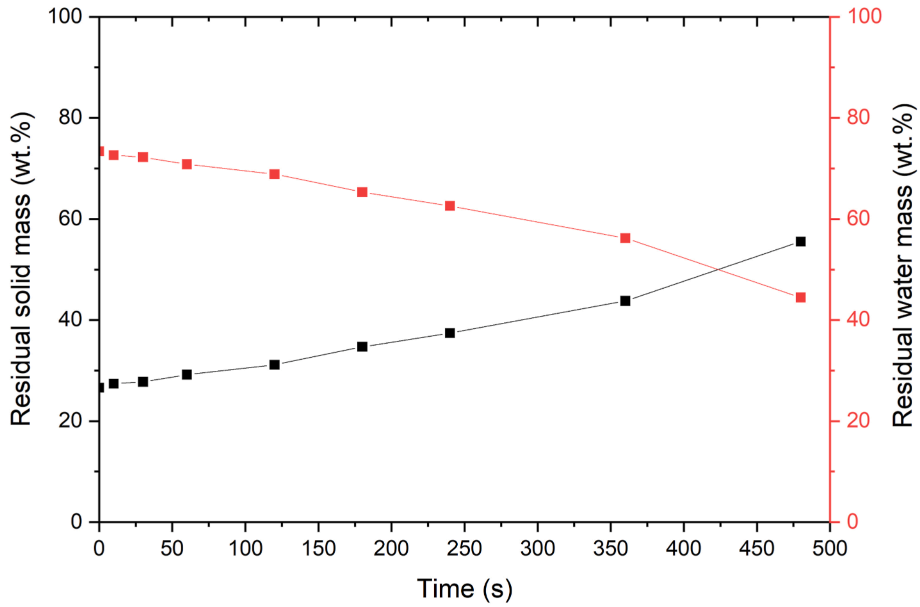

Fig. 2. Percentage of moisture and solid mass fraction in the recycled Arabic gum as function of the drying time after the thermal treatment at 105 °C.

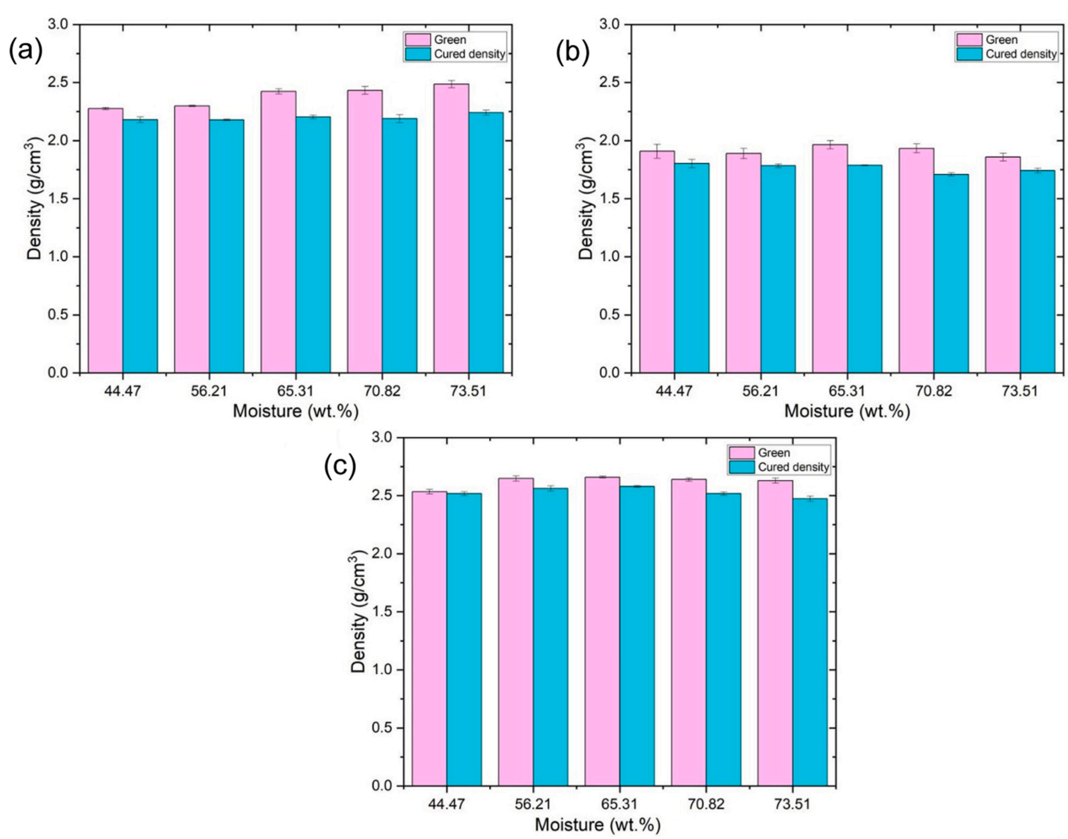

Fig. 3. Green and cured density of briquettes as function of moisture content inside the recycled Arabic gum (a) MS_OP750; (b) MS_OP350; (c) MS_CFD.

insights regarding the low density and worse agglomeration of MS_OP350 when bounded with the binder containing 72.82 wt% moisture (1.71 g cm^{-3}), as this mixture required more time to reach the target pressure (140 s more) (Fig. 4b). The amount of water was sufficiently low to avoid the previous problem of incompressibility, but it was large enough to act as a lubricant between the particles, facilitating their rearrangement and settling (Patil et al., 2009). The large quantity of water improved the way particles were accommodated, which could be arranged differently during the compression stage. Consequently, more time was required for the internal resistance that triggered the pressure increase to develop. Conversely, progressively reducing the water content increased inter-particle friction, resulting in higher material resistance and enabling the target agglomeration pressure to be reached more quickly (Emami & Tabil, 2008). identified the friction coefficient as an important parameter affecting the compressibility of the particles. In fact, increasing the drying time, the loading curves

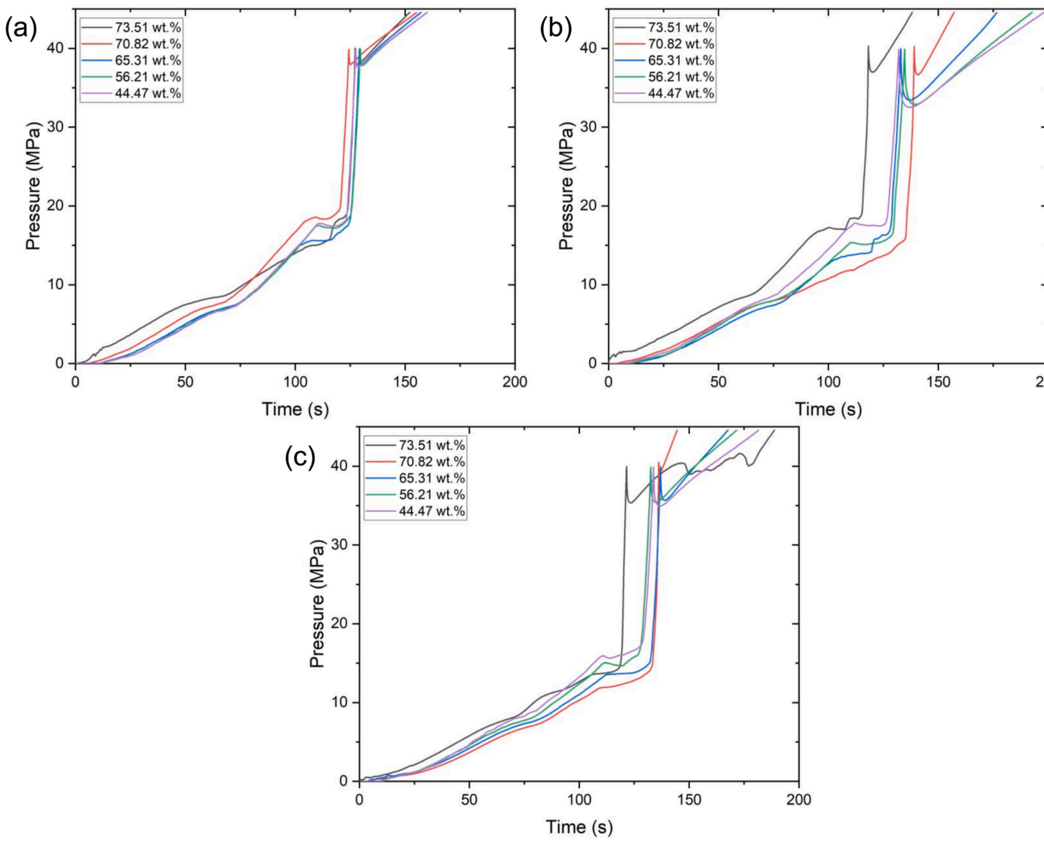

Fig. 4. Loading history of briquettes (a) MS_OP750; (b) MS_OP350; (c) MS_CFD.

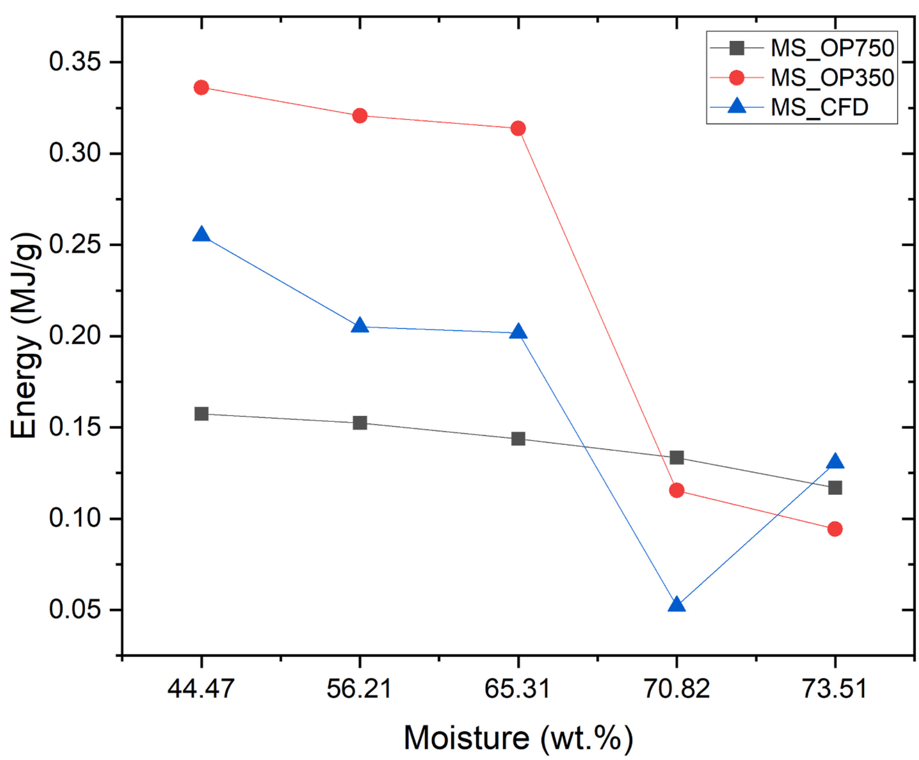

Fig. 5. Energy required for briquetting as function of moisture inside the recycled Arabic gum.

shifted toward lower compression time due to the increase in the resistance of particles accommodation.

The influence of friction during compaction became even clearer when the energy required for briquetting was considered (Fig. 5). This parameter was calculated as the mechanical work needed to compress powder during briquetting (Tumuluru, 2010) and subsequently normalized with respect to the mass of the produced briquette.

With the exception of MS_CFD bounded with 73.51 wt% of moisture in the recycled Arabic gum, which was considered as an outlier, the progressive reduction of water content in the binder led to a gradual increase in the energy required for agglomeration. Water indeed acted as a lubricant between particles, reducing interparticle friction and facilitating their rearrangement during compression (Patil et al., 2009). As the moisture content decreased, this lubricating effect was progressively lost, resulting in higher frictional resistance and therefore greater mechanical work required to reach the target compaction pressure.

However, the magnitude of this effect strongly depended on the interaction between water and particles. In the case of hydrophilic OP750, the energy variation remained relatively limited at 34%. These particles readily absorbed water, ensuring that the available moisture was distributed more uniformly throughout the mixture. As a result, most of the particle surfaces became wetted. This facilitated sliding of the particles, improved packing efficiency and mitigated the increase in friction during compaction. Conversely, hydrophobic materials, such as OP350 and CFD, differently interacted with water because they repelled excess moisture rather than absorb it. When the binder contained higher water contents, the excessive moisture could still provide a certain lubricating effect within the mixture. However, the reduced amount of water was no longer sufficient to properly wet the particle surfaces. As a consequence, particle-particle contacts occurred under poorly lubricated conditions, significantly increasing internal friction within the powder bed. This resulted in a greater resistance to particle rearrangement and ultimately required higher compaction energy to successfully agglomerate the briquettes. However, this was related to the level of hydrophobicity of the powder. OP350 had a contact angle that was 25% higher than that of CFD; consequently, it rejected more water and required an energy variation of 169% more than the ironmaking waste to compress a mixture containing the binder with 44.47 wt% of water instead of 73.51 wt% (energy variation of 256% for MS_OP350 and 95% for MS_CFD between the energies necessary to compress a mixture containing a recycled Arabic gum with 44.47 and 73.51 wt% of moisture).

3.1.1. Mechanical characterization

The results of the mechanical characterization are reported in Table 4.

All the MS_OP750 mixtures exceeded the industrial IRI thresholds of 50 (Richards, 1990), surviving to 10 drops each. AIRI values of 760.66 and 733.41 were obtained for the undried mixture and the mixture containing the binder with 70.82 wt% of moisture, respectively, indicating a higher impact resistance and a reduced tendency to generate fines compared to the other tested conditions.

Similarly, MS_CFD exhibited IRI values of 1000 when bounded with recycled Arabic gum with moisture content greater than 65.31 wt%, but, when the water content in the binder was further reduced, the briquettes withstood a lower number of drops, resulting in IRI values of 405.56 and 283.33 when the binder contains 56.21 and 44.47 wt% of moisture, respectively. A balance in the water content was therefore required. When the amount of water in the system was too low, the briquettes became more brittle, which negatively affected their resistance to impact (Ding & Yue, 2018). Conversely, higher water content increased the elasticity of the briquette structure and enhanced the cohesive forces among the particles, ultimately improving the overall durability of the agglomerates (Olugbade et al., 2019). Hence, an adequate moisture level (water-solid ratio of 1.88:1) played a key role in maintaining a suitable compromise between mechanical strength and structural flexibility.

A Bonferroni post-hoc test (provided in Supplementary material) performed on the drop test results confirmed that the MS_OP750 and MS_CFD briquettes agglomerated with recycled Arabic gum containing 56.21 and 44.47 wt% of water exhibited significantly lower performance. In contrast, no statistically significant differences were observed among the other drying conditions. Excluding hence these dried solutions, the drop test was not a discriminating test for distinguishing the effectiveness of different drying times within the same mixture.

Considering the compression test (Table 4), the optimal moisture content was 65.31 wt% for both the MS_OP750 and MS_CFD mixtures, which showed the highest UCS of 6.29 and 18.02 MPa, respectively. In both cases, the UCS increased as the moisture content decreased up to 65.31 wt% (Barisetty et al., 2020). However, any further reduction in water in MS_OP750 led to a decline in compressive strength (2.81 MPa when the recycled Arabic gum contained 44.47 wt% of moisture), reflecting the negative effect of insufficient moisture on particle cohesion and briquette integrity (Olugbade et al., 2019).

The benchmark for industrial and domestic applications was set at 350 kPa (Richards, 1990), corresponding to the maximum load occurring during loader bucket filling (Abdelrahim et al., 2021). According to (Borowski et al., 2017), briquettes with compressive strength below 1 MPa were unsuitable for transport and storage. For metallurgical use, the cold compressive strength (CCS) should be at least 120 N pellet^{-1}, with values of 300 N pellet^{-1} were required for specific shaft furnace processes, such as Tecnored process (Mantovani & Cyro, 2000). Considering these thresholds, both MS_OP750 and MS_CFD were suitable for industrial applications, as their UCS values were above 1 MPa (Borowski et al., 2017). However, for application inside a converter, the minimum CCS requirement was 9.8 MPa (Barisetty et al., 2020), hence only MS_CFD could be theoretically charged.

All the MS_OP350 briquettes, instead, broke during the drop test, failing to maintain a sufficient level of integrity to proceed to the compression test. Although the lower density obtained (1.79 g cm^{-3})

Table 4
Mechanical characterization of briquettes ("n.d." means not done because the briquettes did not survive to drop test).

Sample	Moisture content	IRI	AIRI	Number of drops	UCS [MPa]
MS_OP750	73.5 wt%	1000.00 ± 0.00	760.66 ± 26.71	10.00 ± 0.00	5.31 ± 2.27
	70.82 wt%	1000.00 ± 0.00	733.41 ± 51.40	10.00 ± 0.00	6.09 ± 1.40
	65.31 wt%	1000.00 ± 0.00	617.10 ± 81.30	10.00 ± 0.00	6.29 ± 1.44
	56.21 wt%	1000.00 ± 0.00	517.65 ± 48.80	10.00 ± 0.00	5.06 ± 1.22
	44.47 wt%	1000.00 ± 0.00	52.49 ± 48.20	10.00 ± 0.00	2.81 ± 0.23
MS_OP350	73.5 wt%	216.67 ± 104.08	100.35 ± 23.62	4.33 ± 2.08	n.d.
	70.82 wt%	272.22 ± 67.36	48.59 ± 51.40	7.00 ± 0.00	n.d.
	65.31 wt%	283.33 ± 104.08	20.72 ± 35.88	6.33 ± 1.53	n.d.
	56.21 wt%	266.67 ± 104.08	24.26 ± 42.02	5.33 ± 2.08	n.d.
	44.47 wt%	94.44 ± 41.94	3.57 ± 6.18	2.67 ± 1.53	n.d.
MS_CFD	73.5 wt%	1000.00 ± 0.00	728.39 ± 67.21	10.00 ± 0.00	8.35 ± 1.25
	70.82 wt%	1000.00 ± 0.00	593.29 ± 11.30	10.00 ± 0.00	15.67 ± 4.39
	65.31 wt%	1000.00 ± 0.00	604.64 ± 79.95	10.00 ± 0.00	18.02 ± 0.76
	56.21 wt%	405.56 ± 122.85	14.51 ± 16.63	9.00 ± 1.00	n.d.
	44.47 wt%	283.33 ± 76.38	7.91 ± 13.69	5.67 ± 1.53	n.d.

negatively affected the mechanical resistance (Sen et al., 2016), they all exceed the threshold surviving to 4 drops and showing IRI higher than 50 (Richards, 1990). Consequently, the dried recycled Arabic gum containing 65.31% of moisture was adopted for the MS_OP350 mixture as well, aligning it with the optimal conditions identified for the other mixtures. The choice of a common water content facilitated the standardization of the process and its scalable implementation in an industrial context, where defining a single, well-controlled drying time is a critical prerequisite for ensuring consistent product quality, reliable mechanical performance, and uninterrupted production continuity. By establishing such a reproducible parameter, the process would become more predictable and manageable, thereby supporting both operational efficiency and quality assurance in large-scale manufacturing.

Overall, moisture content of 65.31 wt% in the recycled Arabic gum proved to be the most favorable condition, because the water-solid ratio was effectively balanced, resulting in consistent mechanical responses across different mixtures, including both OP750 and CFD. The drop test confirmed sufficient impact resistance, while compressive strength reached its maximum, establishing the water-solid ratio of 1.88:1 as the optimal value for densification and cohesion. It differed by only 0.1% from the ratio previously established using natural Arabic gum to agglomerate BOFD and BFS by (Scolari et al., 2026). This remarkable consistency demonstrated that recycled Arabic gum was capable of reproducing the ideal water-solid balance. Moreover, the favorable obtained results across multiple iron-bearing matrices strongly suggested that the water-solid ratio of 1.88:1 condition represents a broadly applicable formulation rather than a system-specific optimum. In this way, the study provided robust proof that recycled Arabic gum can successfully replace natural gum and maintain mechanical reliability, while significantly reducing the high costs associated with the natural binder ((tridge.,) "https://www.tridge.com/intelligences/arabic-gum/price; Last Access 01/09/2025" n. d.), and supporting the development of more sustainable and economically viable self-reducing briquette production.

3.2. Comparison between recycled Arabic gum and corn starch

3.2.1. Mechanical characterization

The effect of the binder in the densification of the briquettes depended on the mixture used. As shown in Fig. 6(a), the improvement in cured density using starch was approximately 14% in presence of biochar (2.20 vs. 2.56 g cm^{-3} for MS_OP750 and 1.79 vs. 2.16 g cm^{-3} for MS_OP350), while the recycled Arabic gum increased the density of MS_CFD by 4% (2.66 vs. 2.56 g cm^{-3}) (Scolari et al., 2026). obtained the same 4% increase in density by agglomerating fine BOFD with BFS, also given the chemical and mineralogical similarity between CFD and BFS.

The finer PSD of CFD (Table 3) probably reduced the inter-particle voids and limited water evaporation during the curing period. This promoted the formation of a network of microporosity throughout the briquette and resulted in higher density using the liquid binder. By contrast, the use of coarser particles, such as OP750 and OP350, enabled the excess water in the recycled Arabic gum to be expelled more easily during the curing process. This resulted in lower final densities. Therefore, the interplay between particle size distribution and binder characteristics was confirmed as a key factor in densification.

The improvement and worsening in density according to the specific mixture were also supported by literature data. Briquettes made of BOFD and secondary dust showed the same densifications independently from the binder (Scolari et al., 2026). Briquettes made of *A. indica* sawdust with starch showed a density 1.28 times higher than with Arabic gum (Sotannde et al., 2010), while an improvement in densification (1.38 times) using fine particles of charcoal was obtained substituting starch with Arabic gum (Sotannde et al., 2009).

The mechanical results of drop and compression tests are reported in Table 5. Although higher density was achieved with MS_OP750_CS and MS_OP350_CS, the Arabic gum increased the impact resistance of all the mixtures. The IRI indeed increased by 30, 277 and 424% with OP750, OP350 and CFD, respectively. Considering the IRI, both MS_OP750_AG and MS_CFD_AG showed the highest impact resistance, reaching the

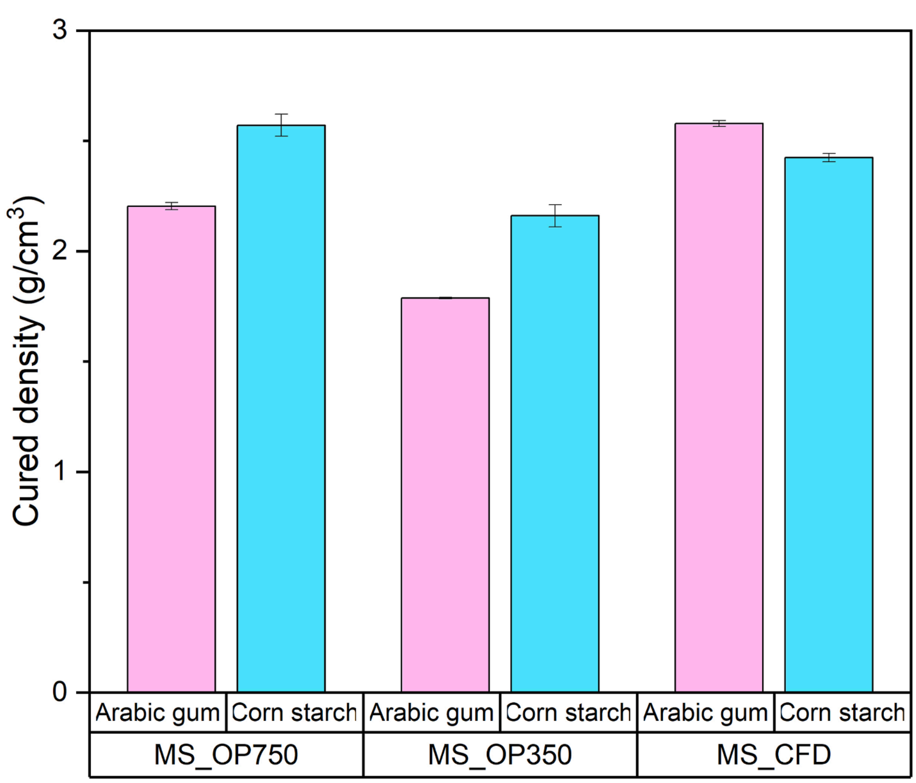

Fig. 6. Green and cured density of briquettes with starch and recycled Arabic gum. Data of MS_OP750_CS and MS_OP350_CS were collected from (Dall'Osto et al., 2024).

maximum achievable value of 1000. Since this value represents the upper limit of the IRI scale, a comparison based on the AIRI is also necessary to provide a more accurate assessment of the briquettes' impact resistance. Indeed, the AIRI is more sensitive in distinguishing the behavior of agglomerates when the IRI reaches its maximum value. The superior performance of recycled Arabic gum was further confirmed by the increase in AIRI, which improved by 16% for OP750 and by 2496% for CFD. This enhancement can be attributed to the higher amount of free water present in the recycled Arabic gum, which promoted the initial bonding between fine particles and consequently resulted in greater impact resistance (Patil et al., 2009; Sen et al., 2016). However, MS_OP350_AG could not guarantee the briquettes' survival up to 10 drops, even though recycled Arabic gum increased IRI by almost three times. The limited absolute value of density (1.79 g cm^{-3}) and the resulting worse agglomeration indeed intrinsically reduced the mechanical resistance of the briquettes (Sen et al., 2016). The behavior of MS_CFD was instead consistent with the improvement of density using the recycled Arabic gum. MS_CFD_AG not only survived to 10 drops but also remained compact releasing a limited quantity of fines, having AIRI of 604.64.

Although the compression tests on MS_OP750_CS and MS_OP350_CS were performed on raw briquettes and did not follow the drop test procedure, the results (Table 5) were compared with those of the same mixture that had been bound with recycled Arabic gum and had previously been dropped (Scolari, Dall'Osto, et al., 2025). indeed demonstrated that the UCS was independent from the previous drop test, hence the values were considered comparable.

Once again, the mechanical response of the briquettes was strongly dependent on the binder used and on the specific mixture tested. In particular, the compressive resistance of MS_OP750 decreased by 45.59% when recycled Arabic gum was used instead of starch. The MS_OP350_CS had an acceptable UCS of 3.91 MPa for industrial applications (Borowski et al., 2017), but not suitable inside a converter being lower than 9.8 MPa (Barisetty et al., 2020). Finally, the UCS of MS_CFD_AG was 84% higher than the most restrictive benchmark (Barisetty et al., 2020), and comparable only with the optimized mixture of BOFD and BFS agglomerated with starch and double content of water (Scolari, Mombelli, et al., 2025). These different resistance behaviors further confirmed that the mechanical performance of the agglomerates cannot be generalized and must be evaluated for each specific binder-mixture combination.

The reduction in mechanical strength observed for MS_OP750_AG is likely associated with differences in particle arrangement induced by the binder during the agglomeration stage (Fig. 7). Such variations altered the packing structure of the particles and, consequently, the formation of the internal load-bearing network responsible for transmitting stresses within the briquette. When Arabic gum was employed, the mill scale was predominantly aligned parallel to the direction of the briquetting load (Fig. 7a–c). This orientation reduced the effective resistant cross-section of the particles under compression, making the agglomerates more susceptible to mechanical failure. Since the compression test was performed under controlled displacement of 15 mm min^{-1}, the smaller load-bearing area resulted in higher effective stress acting on the particle framework, ultimately lowering the compressive resistance of the briquettes (Emami & Tabil, 2008).

By contrast, when starch was used as a binder, the particles were arranged more orthogonally to the direction of compaction (Fig. 7d–f). This configuration increased the effective resistance section exposed to the applied load, hence enabling its distribution over a larger surface area of the particles, thereby enhancing the mechanical strength of the briquettes.

These differences in particle orientation were caused by the two binders having different rheological behavior during the agglomeration process (Arabic gum solution at 25% is characterized by 100 cP (Idirs, 2017), while gelatinized starch reached viscosity one order of magnitude higher (Jin et al., 2019)). Starch formed a gel-like matrix characterized by relatively high viscosity, which limited the mobility of solid particles during compaction. Consequently, the mill scale remained embedded within the viscous network, adopting a stable orientation largely independent of the compaction direction. High-viscosity fluids were known to dampen particle motion by reducing the magnitude of inter-particle contact stresses and limiting particle rearrangement and percolation within the mixture (Carotenuto, 2023; Cui et al., 2021). This behavior favored the formation of cohesive liquid bridges between particles and suppressed particle velocity fluctuations, thereby stabilizing the particle framework during densification (Cui et al., 2021). On the contrary, Arabic gum, which behaved similarly to an aqueous solution, allowed greater particle mobility during compaction. Under the action of the applied load, the particles could more easily slide and reorient within the mixture, progressively aligning along the direction of pressure application. This enhanced mobility ultimately favored the formation of a particle structure less effective at resisting compressive stresses.

Although the particles orientation reduces the compression resistance of the briquette, the compact packing and fine PSD of the cupola dust favored a UCS of 18.02 MPa for MS_CFD_AG (Table 5). Fig. 7c shows indeed a more compact and tight morphology than Fig. 7f, highlighting a porosity of 29% with the Arabic gum, which was increased to 33% with starch. As already observed by (Scolari et al., 2026) a wider PSD favored a homogeneous arrangement of particles which resulted in a better agglomeration. The voids between coarse elements are easily filled by the smallest fraction. This increases cohesion, resulting in the enhancement of mechanical properties (Pang et al., 2019). Although the same improvement in particles arrangement was obtained with MS_OP750_AG and MS_OP350_AG (porosity increased by 13 and 19% compared to starch counterpart, respectively), only the small particle size of CFD led to a very high compression resistance. The small PSD indeed favored the increase in number of stronger contact forces between particles (Zepeda-Cepeda et al., 2021; Zhu et al., 2025).

3.2.2. Metallurgical characterization

The swelling behavior of the briquettes heat treated at 750, 900, 1050 and 1200 °C is shown in Fig. 8. The replacement of starch with recycled Arabic gum effectively solved the catastrophic swelling problem observed for MS_OP750_CS and MS_OP350_CS. Maintaining dimensional stability during thermal treatment is a critical requirement for self-reducing agglomerates. This is because abnormal or catastrophic swelling can lead to a severe loss of mechanical integrity. This is typically defined as an expansion exceeding 20%, that ultimately promotes degradation and disintegration of the briquette (Mantovani et al., 2002).

Table 5
Mechanical results of briquettes agglomerated with both binders (* refers to compression test performed on raw briquettes not previously subject to drop test) ("n.d." means not done because the briquettes did not survive to drop test). Data of MS_OP750_CS and MS_OP350_CS were collected from (Dall'Osto et al., 2024).

Binder	Mixture	IRI	AIRI	Number of drops	UCS [MPa]
Arabic gum	MS_OP750	1000.00 ± 0.00	617.10 ± 81.30	10.00 ± 0.00	6.29 ± 1.44
	MS_OP350	283.33 ± 104.08	20.72 ± 35.88	6.33 ± 1.53	n.d.
	MS_CFD	1000.00 ± 0.00	604.64 ± 79.95	10.00 ± 0.00	18.02 ± 0.76
Corn starch	MS_OP750	766.70 ± 230.20	531.53 ± 347.08	9.50 ± 0.50	11.56* ± 2.74
	MS_OP350	75.00 ± 22.50	0.00 ± 0.00	3.00 ± 2.00	3.91* ± 0.56
	MS_CFD	191.67 ± 142.16	23.92 ± 33.03	4.33 ± 2.31	n.d.

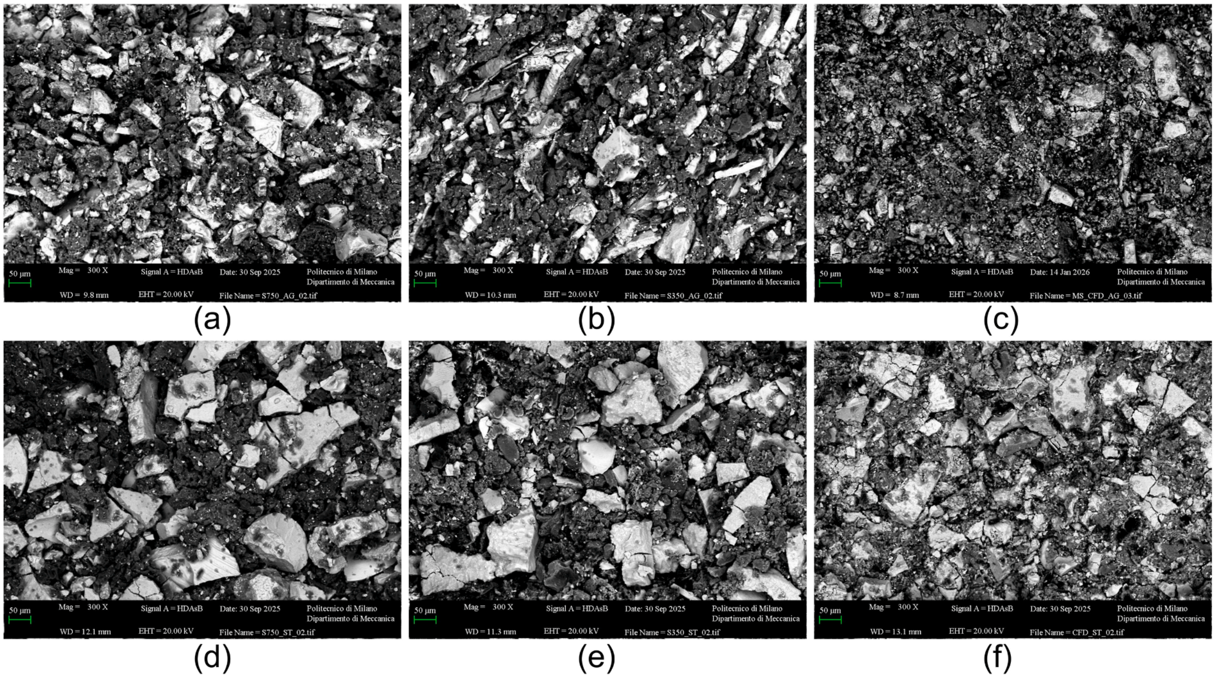

Fig. 7. BSE images of cured briquettes (a) MS_OP750_AG; (b) MS_OP350_ AG; (c) MS_CFD_ AG; (d) MS_OP750_CS; (e) MS_OP350_CS; (f) MS_CFD_CS. The direction of load compression was internal to the plane.

MS_OP750_CS already exhibited noticeable swelling at 750 °C (16.55%), which dramatically increased to 153.62% at 900 °C, indicating a clear case of catastrophic expansion at the typical swelling temperature (Maneesh Singh & Bjorkman, 2004). In contrast, the briquettes produced with recycled Arabic gum maintained a high level of dimensional stability up to 900 °C with nearly null volume variation. At 1050 °C, MS_OP750_AG exhibited moderate expansion of 8.67%. This is only around 10% of the swelling observed in starch-based briquettes at the same temperature (86.72%) and is therefore well below the threshold typically associated with catastrophic swelling. Finally, at 1200 °C, shrinkage was observed in both cases, at −38.67% for the Arabic gum briquettes and −4.00% for the starch-based briquettes.

Similar behavior was observed with MS_OP350. MS_OP350_CS swelled between 750 °C and 1050 °C (with a maximum peak of 99.02%

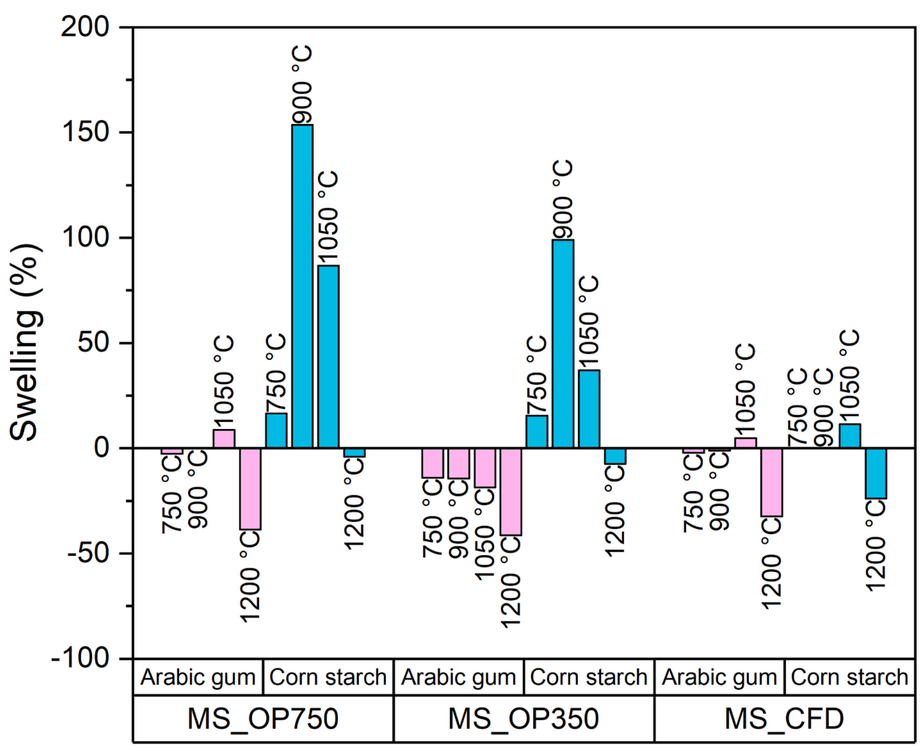

Fig. 8. Swelling behavior of briquettes thermally treated at 750, 900, 1050 and 1200 °C. Data of MS_OP750_CS and MS_OP350_CS were collected from (Dall'Osto et al., 2024).

at 900 °C) and then showed shrinkage at 1200 °C (−7.37%). Arabic gum instead not only completely hindered any swelling phenomena observed in MS_OP350_CS, but it also increased the shrinkage at each temperature (from −14.09% at 750 °C to −41.25% at 1200 °C). The positive effect of shrinkage was generally an increase in strength, due to the interconnection of iron particles and the development of a connected slag network, which was favored during volume reduction (Somerville, 2016; Wu et al., 2023).

The swelling behavior of MS_CFD was instead similar regardless of the binder used. No volume variation was observed up to 900 °C, no-catastrophic swelling occurred at 1050 °C (MS_CFD_AG 4.77% and MS_CFD_CS 11.52%) and shrinkage occurred at 1200 °C (MS_CFD_AG −32.30 and MS_CFD_CS −23.87%).

As already observed by Scolari et al. (2026) during the thermal treatments, Arabic gum promoted the densification rather than expansion, solving the problem of catastrophic swelling observed for the briquettes bounded with corn starch. This alternative binder therefore ensured that briquettes made of any material remained within the safety limits for industrial operations at high temperatures (<20%) (Andersson et al., 2019), making an optimal choice from a high-temperature mechanical point of view (Singh & Bjorkman, 2004).

Fig. 9 shows the effect of the binder in the metallurgical behavior of briquettes.

The RD was higher with Arabic gum only at 750 °C for MS_OP350 and MS_OP750. Although, OP350 was in general more reactive up to 900 °C (RD 81.91 and 26.77% higher for MS_OP350_AG and MS_OP350_CS than those with OP750) due to the high amount of volatile matter (62.55 wt%) (Wei et al., 2016), both MS_OP750 and MS_OP350 mixtures showed a more effective reduction capacity with starch at any other temperatures. The swelling of the briquettes given by the starch increased the internal porosity within the briquette favoring the presence of CO due to larger reaction surface (Bagatini et al., 2020), resulting into higher degree of reduction. On the contrary, the shrinkage observed with Arabic gum led to an occlusion of the internal porosity network, thus limiting the previous effect. The shrinkage observed in Arabic gum-containing briquettes may be associated with the combined effect of the additional carbon supplied by the binder (nearly 2.4 wt% more than stoichiometric carbon), which can promote a more extensive reduction and subsequent densification, and the presence of Si-Ca-S inorganic residues (Scolari et al., 2026) (6 wt% residues at 600 °C) that may favor liquid-phase slag formation. However, the volumetric evolution of self-reducing briquettes during thermal treatment is governed by multiple interacting phenomena, including reduction kinetics, gas generation, sintering, and slag development.

A further explanation for the limited RD observed when using Arabic gum lies in the incomplete removal of the binder during the process. In fact, a fraction of the Arabic gum is probably likely retained within the sample, rather than being entirely eliminated. As a consequence, the theoretically expected mass loss should be slightly lower than the value calculated under the assumption of complete binder removal, since not all of the initial binder content effectively contributed to the measured mass loss. This assumption was further supported by the better mechanical stability achieved with the Arabic gum, despite (Koohestani et al., 2025) sustained the disappearance of the organic binder after the thermal treatments.

On the contrary, MS_CFD_AG showed a slightly higher degree of reduction up to 1050 °C (74.63% compared to 70.80% with starch). However, the reduction degree obtained with recycled Arabic gum at 1200 °C was approximately 4% lower than that achieved with starch. The improved reduction observed at intermediate temperatures when recycled Arabic gum is used as a binder can be attributed to the particles having more intimate contact with each other (Fig. 7), which likely enhanced gas-solid interactions and facilitated the progression of reduction reactions (Liu et al., 2024). At higher temperatures, however, the complete decomposition of starch may leave a more fragmented and porous internal structure, which could promote gas diffusion and allow the residual oxides to be reduced more efficiently.

Despite these local differences, the variations in RD observed at high temperature between the two binders remained within the experimental error of 5%, except for MS_OP350 up to 900 °C. The choice of binder

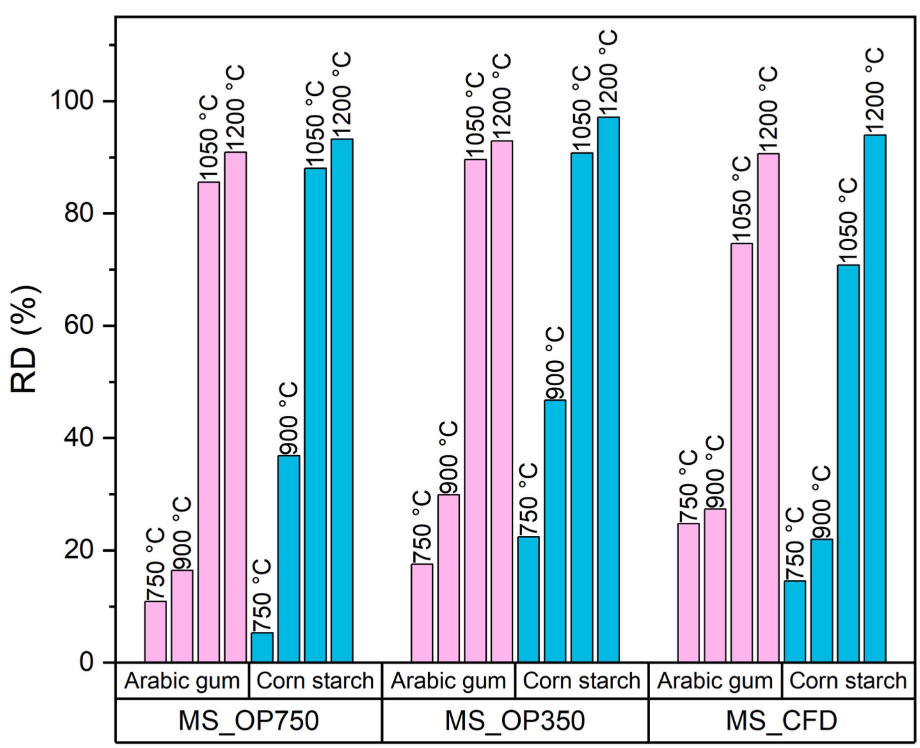

Fig. 9. Degree of reduction of briquettes thermally treated at 750, 900, 1050, 1200 °C. Data of MS_OP750_CS and MS_OP350_CS were collected from (Dall'Osto et al., 2024).

hence did not significantly affect the proposed metallurgical property of the briquettes. Consequently, Arabic gum can be considered fully suitable from a metallurgical standpoint across all the mixtures investigated, confirming that its substitution for starch did not compromise the reduction behavior of the self-reducing agglomerates.

To highlight the sigmoidal trend of the DR as function of temperature of each mixture, the experimental data were interpolated using a variant of the Avrami model (Fanfoni & Tomellini, 1998) according to Eq. (10). It should be noted that the Avrami equation was employed exclusively as an empirical fitting function to describe the sigmoidal evolution of the reduction degree with temperature and to facilitate comparison among the investigated formulations. No kinetic interpretation of the fitting parameters is intended.

$$\ln\left[\ln\left(\frac{1}{1-\mathrm{RD}}\right)\right] = \ln(K) + n\ln(T) \tag{10}$$

where the time variable was replaced by the absolute reduction temperature T (expressed in Kelvin), assuming that the measured RD corresponds to the maximum value achievable for each heat treatment condition, K is a constant parameter and n is the slope of the regression.

Fig. 10 confirmed that the RD obtained using olive pomace were not significantly affected by the type of binder used. The slope of the regression line was instead more dependent on the mixture. MS_OP750 was indeed characterized by a mean slope value around 10.10, while MS_OP350 by 7.72. As already demonstrated by Dall'Osto et al. (2024), a higher FC content increased the value of n, thereby enhancing the capacity of the system to recover iron at elevated temperatures through direct carbothermal reduction. OP750 indeed contains approximately 47% more FC than OP350, providing a larger reservoir of reactive carbon available to sustain the reduction reactions at high temperature. This greater carbon availability favored the direct reduction of iron oxides and led the reaction toward more advanced stage of metallization. As a result, the briquettes produced with OP350 exhibited a slightly lower degree of reduction at 1200 °C, with RD values nearly 3% and 5% lower than those measured for MS_OP750_AG and MS_OP750_CS, respectively. Slightly higher slope variation using the different binders (8.26 with starch and 6.26 with recycled Arabic gum) were instead obtained using CFD.

The value of the intercept was also affected by the mixture selected. OP750 led to a ln (K) equal to nearly −72.47, OP350 to −55.07 and CFD of −52.10. Considering the olive pomaces, higher VM in OP350 (+21%) gave higher regression constant ln(K), promoting the RD at low temperatures due to gasification. In addition, the close contact between MS and CFD, favored faster reduction kinetics in the 750-1050 °C range. The highest intercept (−44.867) was indeed obtained by MS_CFD_AG which resulted extremely compacted and uniform (Fig. 7).

The slight, non-significant effect of the binder change on metallurgical performance was also confirmed by the smelting behavior at 1400 °C. MS_OP750_AG appeared as a hemispherical shape (Fig. 11a), showing a large internal cavity opening on the upper part of the briquette itself, with a large number of coalescences with dimensions smaller than 2 mm. From inside the cavity, a large number of spherical ferrous particles were collected, with a diameter smaller than 0.5 mm, with the exception of a few larger particles. The slightly higher RD obtained with MS_OP750_CS (nearly 3%) justified the complete smelting obtained by Dall'Osto et al. (2024).

Both MS_OP350_CS and MS_OP350_AG (Fig. 11b) showed instead shrinkage in a solid, highly metallized structure. Similar shape was obtained with both MS_CFD mixtures (Fig. 11c and d). Despite the internal cavity, the high metallization was visible by eye.

Complete smelting was hence observed only for the mixture characterized by an n value greater than 10 (MS_OP750_CS). As the value of n decreased, the slope of the regression curves progressively flattened, indicating a slower progression of the reduction reactions and a reduced tendency toward full melting. Slope of 9.29 indeed led to a partial smelting since some slag droplets remained attach to the external shell. Further reducing n, the briquettes preserved their original shape during the thermal treatment showing only the expected shrinkage. The internal structure, however, exhibited a network of pores and cavities generated by the evolution of gaseous species during the reduction process. These voids reflected the progressive removal of oxygen from

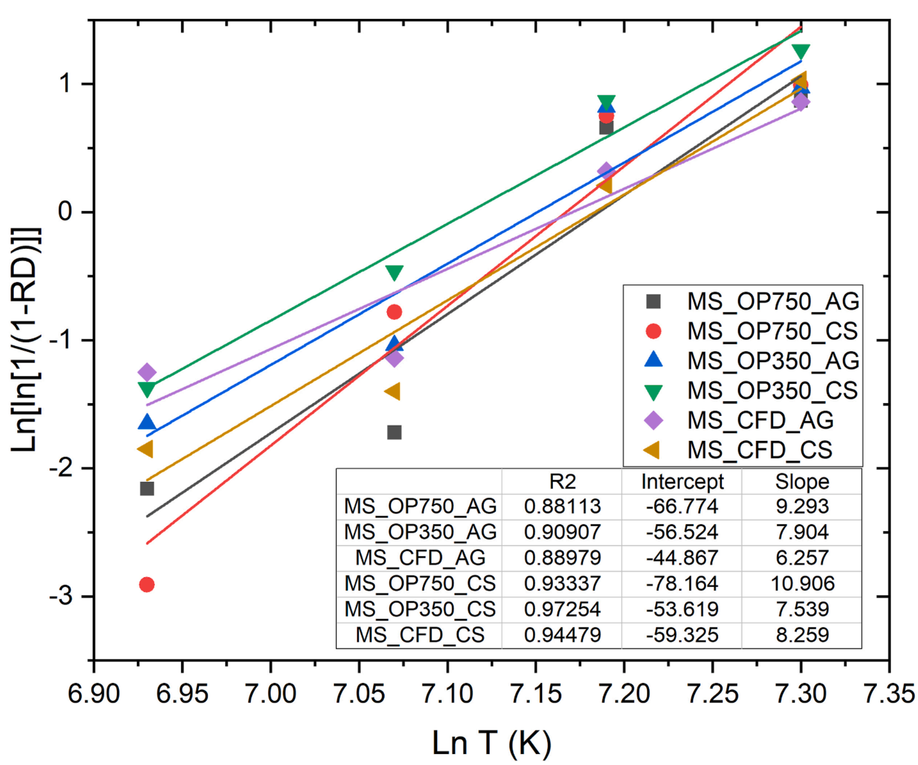

Fig. 10. Linearized plot of DR according to temperature. Data of MS_OP750_CS and MS_OP350_CS were collected from (Dall'Osto et al., 2024).

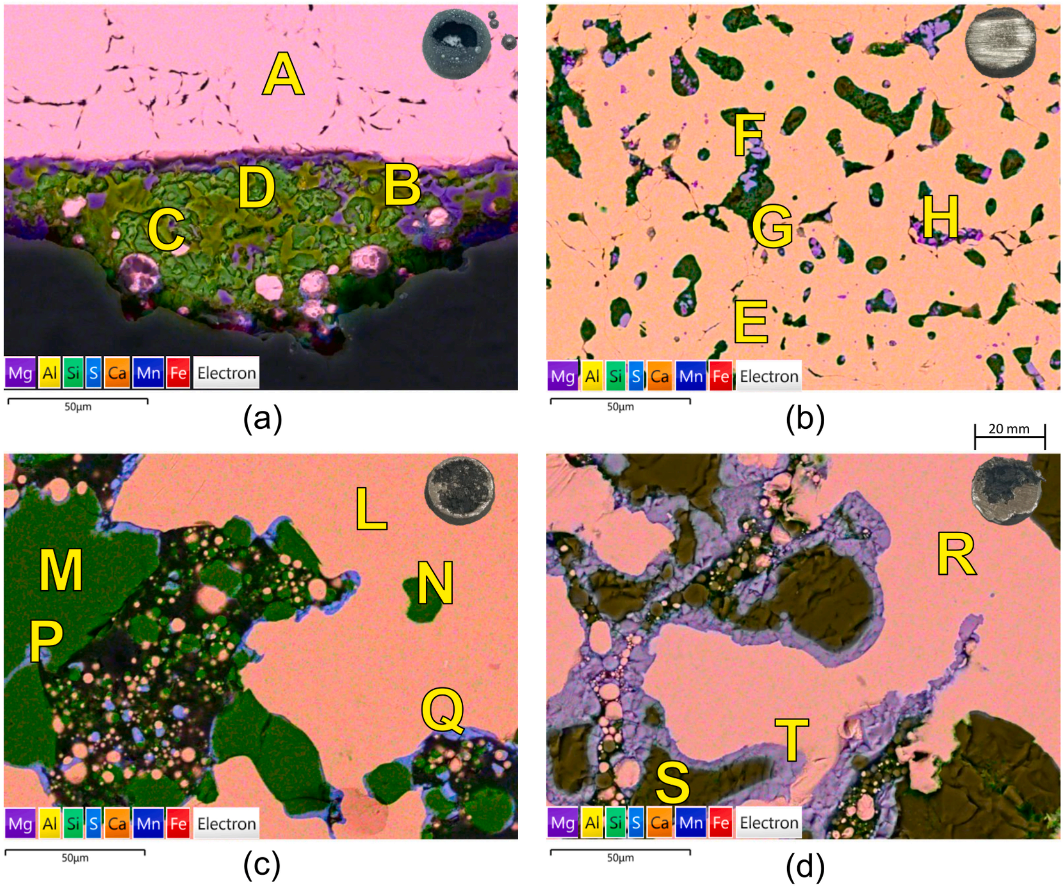

Fig. 11. SEM images of briquettes thermally treated at 1400 °C (a) MS_OP750_AG; (b) MS_OP350_AG; (c) MS_CFD_AG; (d) MS_CFD_CS.

the iron oxides and the release of reaction gases, which expanded within the agglomerate without leading to complete structural collapse or melting of the briquette (Dall'Osto et al., 2024).

SEM-EDS analyses were performed to evaluate whether the type of binder influenced the chemical composition and microstructure of the smelted briquettes (detailed spectra are reported in supplementary materials). MS_OP750_AG developed a cast iron free from both sulfur and phosphorus (A), although some slag remained attached to the metallic phase. This slag was mainly composed of gehlenite ($Ca_2Al_2SiO_7$ - B), monticellite ($CaMgSiO_4$ - C), and akermanite ($Ca_2MgSi_2O_7$ - D). A very similar morphology was observed in the corresponding starch-based briquettes (MS_OP750_CS), indicating that the binder did not substantially modify the metallurgical products obtained from this mixture (Dall'Osto et al., 2024).

MS_OP350_AG instead showed a metallic matrix (E) containing residual iron oxide (FeO - F), dispersed within a slag phase where potassium was concentrated (G). A comparable microstructure was observed in MS_OP350_CS by Dall'Osto et al. (2024), where islands of metallic and oxidized iron were embedded in a gehlenite-rich slag in which sulfur and phosphorus were dissolved. Although the relatively high sulfur content observed in MS_OP350_AG might suggest a possible contribution from the binder, the absence of phosphorus in the other mixtures indicated that this behavior was more likely related to the intrinsic heterogeneity of the OP350 feedstock rather than to the use of recycled Arabic gum itself.

In MS_CFD_AG, the metallic phase developed into cast iron (L), while the slag was mainly composed of calcium silicates (M-N), in agreement with the chemical composition of CFD. Elements such as Mn and Cr, which in the olive pomace mixtures formed spinel or silicate phases within the slag (H), were instead found segregated along the grain boundaries in manganese-sulfur rich regions (P-Q). MS_CFD_CS showed a similar metallurgical structure, with a cast iron matrix (R) surrounded by calcium silicate slag (S) and MnS (T).

Finally, according to SEM-EDS, the final chemical composition and phase distribution of the reduced products were primarily governed by the characteristics of the mixtures used rather than by the binder. In all the investigated systems, replacing starch with recycled Arabic gum did not significantly alter the chemistry of the metallic phase or the nature of the slag. The binder hence played a limited role in determining the final metallurgical products of the reduction process.

The visual high metallization of all the mixture was confirmed by the DoM reported in Fig. 12.

Both the binders gave a DoM close to 100% with MS_OP750. The efficiency of the reduction process was hence not penalized by the substitution of starch with the recycled Arabic gum and confirmed the excellent metallurgical performances of the system based on OP750. The slightly relative reduction in DoM (1.52%) was due to a partial presence of FeO_x-containing slag still attached to the metallic droplets. On the contrary, the recycled Arabic gum improved both the metallization of MS_OP350 and MS_CFD by 9 and 2%, respectively. The latter difference could be considered experimental errors being lower than 5%, while the former could be associated to the chemical composition of the binder itself. The overall performance of OP350 was indeed limited due to a low amount of FC (31.44 wt%), as previously explained (Wu et al., 2023). Nevertheless, the not complete disappearance and the intrinsic content of carbon in the recycled Arabic gum (dissolved organic carbon of 9.1-16.8 wt% corresponding to 1.8-3.4% additional to stoichiometric carbon) compensated the deficit of the reducing agent promoting a more effective reduction and a higher DoM compared to starch.

Both the binders satisfy the industrial requirement of metallization higher than 76% with any mixtures (Bagatini et al., 2017). The briquettes could hence be used as secondary charge in the main

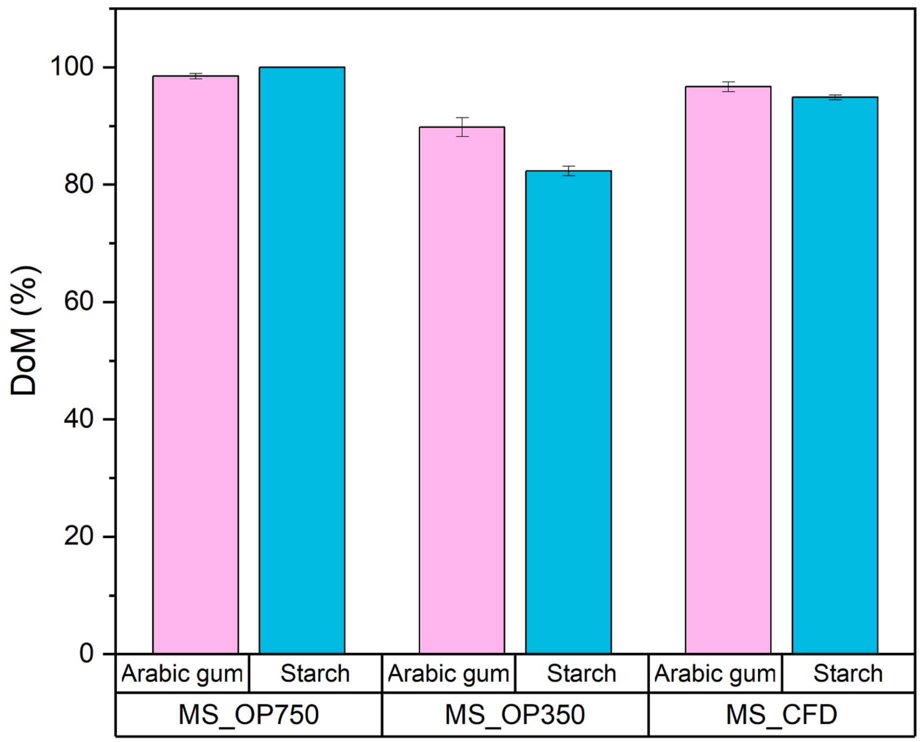

Fig. 12. Degree of metallization of briquettes reduced at 1400 °C. Data of MS_OP750_CS and MS_OP350_CS were collected from (Dall'Osto et al., 2024).

metallurgical processes, without relevant effects on the chemical composition of the bath or on process times (Bagatini et al., 2017).

3.3. Feasibility study

The experimental results confirmed the technical validity of the recycled Arabic gum as a binder for self-reducing briquettes. Considering both the results obtained in this work and those reported by the authors in (Scolari et al., 2026), none of the binder can be universally considered superior; instead, their performance depends on the physical and chemical properties of the raw materials involved.

From a mechanical point of view, briquettes containing coarser reducing agents generally benefited from the use of starch. The use of natural Arabic gum with coarse secondary dust used by Scolari et al. (2026) drastically reduced the IRI from 1000 to 189. A reduction in mechanical resistance was observed also with OP750 since the recycled Arabic gum worsened the UCS by 45.59%. The higher viscosity of starch during agglomeration limited particle mobility and favored a particle arrangement more orthogonal to the compaction direction, increasing the effective load-bearing section within the briquette. This configuration resulted in higher cured densities and improved compressive resistance. In contrast, Arabic gum behaved as a lower-viscosity aqueous solution, allowing greater particle mobility during compaction and promoting particle alignment parallel to the briquetting load. This orientation reduced the effective resistant section and consequently decreased the compressive strength of mixtures such as MS_OP750. However, this behavior did not affect finer particles, which instead reduced the inter-particle voids and limited water evaporation during curing, allowing the binder to form a more effective network of liquid bridges and cohesive interactions. Progressively decreasing the PSD, an improvement in mechanical resistance was observed. OP350 increased its IRI from 75 to 283 and CFD from 192 to 1000, reaching also the highest UCS of 18.02 MPa. This positive effect using the recycled Arabic gum on fine particles was also observed by Scolari et al. (2026), where the IRI of briquettes made of BFS improved by 700%.

From a metallurgical point of view, the different binders did not affect the reduction in terms of chemical composition confirming the suitability to use both starch and the recycled Arabic gum. However, the RD showed possible variations between the two binders, according to the mixture. Using biochar (OP750 and OP350), slightly lower RD values were observed with recycled Arabic gum (3 and 7%, respectively). Steelmaking residues also behaved different although the similar origin and chemical composition. CFD worsened the RD by 4%, while the BFS improved it by 4% (Scolari et al., 2026). However, the variation ranged by 5% is considered as experimental error. Increasing instead the PSD (Yu et al., 2014), neither Arabic gum nor starch were able to overcome the problem of limited contact between carbon and iron oxide, keeping a low reduction capacity (Scolari et al., 2026).

Conversely, the DoM was generally favored when recycled Arabic gum was employed. The additional carbon introduced by the gum increased the reducing potential within the briquette and promoted the conversion of iron oxides into metallic iron with OP350 and CFD (9 and 2% increase in DoM). The 100% DoM achieved with OP750 instead suggested to use starch since it was more prone to favor the smelting. Despite the low variation, recycled Arabic gum solved all the problem of briquette's instability and swelling during the thermal treatment, suggesting its use with any mixture at low temperature.

To sum up, the RD was only marginally affected by the use of recycled Arabic gum or, in some cases, resulted slightly lower than that obtained with starch. This behavior could be attributed to the formulation of the RD parameter itself, which also accounted for the complete disappearance of the organic binder. Since the total decomposition and removal of the binder may not occur under using recycled Arabic gum, the calculated RD can appear slightly reduced. In contrast, the DoM was favored in the presence of recycled Arabic gum because the higher carbon content, introduced by the binder, provided additional reducing power and promoted the reduction of the available iron oxides into metallic iron. The enhanced carbon availability therefore facilitated the reaction process, increasing the fraction of iron present in metallic form.

Considering that the goal of self-reducing briquettes was the complete reduction of iron oxides into metallic iron, the degree of metallization represented the most relevant parameter for evaluating

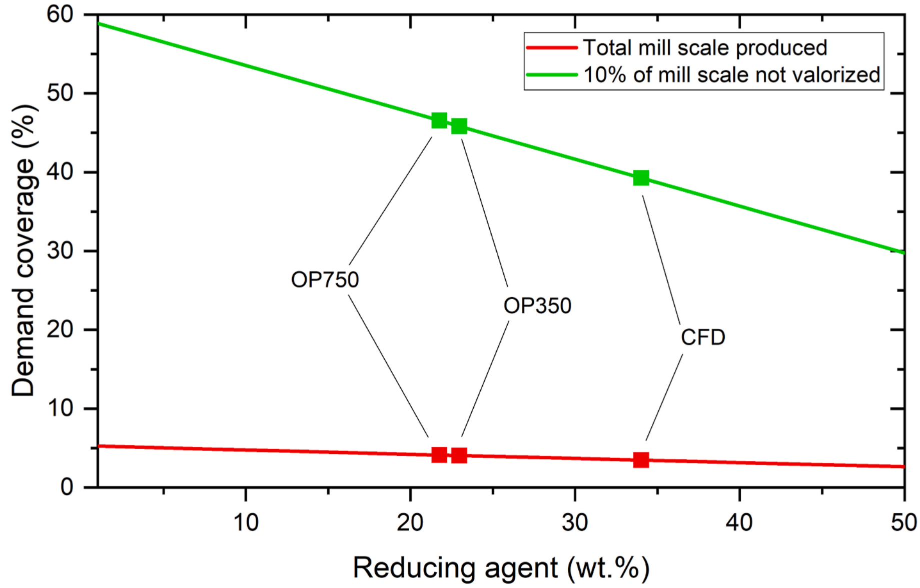

Fig. 13. Demand coverage of recycled Arabic gum to produce briquettes according to the mixture. Red line refers to the limiting condition of using all the mill scale produced. Red line refers to the use of the 10% of mill scale not valorized in other applications.

metallurgical performance. From this perspective, recycled Arabic gum generally performed very well as a binder, as it promoted higher metallization without negatively affecting the overall reduction process.

Overall, the results showed that binder selection should be tailored to the physical characteristics of the mixture, particularly the particle size distribution. Starch proved more suitable for systems containing relatively coarse particles, where its higher viscosity stabilized particle arrangement and improved compressive resistance. In contrast, recycled Arabic gum performed better with finer materials, where its lower viscosity and additional carbon content favored densification and metallurgical performance.

While the present results support the effectiveness of Arabic gum as a binder within the investigated systems, its broader applicability to self-reducing agglomerates still requires further validation across different feedstocks and processing conditions. In this regard, the previous work (Scolari et al., 2026) already provided a first range of tested materials, including steelmaking dust residues. Building on these studies, future investigations will further expand the dataset to other iron-bearing materials or other industrial by-products as red mud, as well as different reducing agents and processing conditions, in order to fully assess the robustness and transferability of the proposed approach.

However, to evaluate the real applicability of the recycled Arabic gum on an industrial scale, it was necessary to assess the availability of the resource, the supply logistics, and the impact on the steel production process. From an economic profile, the use of natural Arabic gum did not offer a competitive advantage compared to starch (7.62 vs. 0.351 $/kg ((tridge.,) "https://www.tridge.com/, access on 15/12/25" n. d.)). Considering instead a processing residue, its procurement cost resulted null or potentially negative, assuming revenues derived from the disposal service offered to wine companies. In addition, although the necessary drying pretreatment entailed an additional energy expenditure, such cost could be significantly reduced by exploiting the various sources of residual waste heat intrinsically available in the different steel cycle (García et al., 2010; Müller et al., 2021; Pauluzzi & Martinis, 2018; Salimbeni et al., 2023).

The Arabic gum was widely employed for the colloidal stabilization of wines, the prevention of coloring matter precipitation, and the improvement of foam stability ((enartis.,) "https://www.enartis.com/wp-content/uploads/2021/05/Enartis-Newsletter-ArabicGum-EN-SA.pdf, access on 18-12-2026" n. d.; Nigen et al., 2019b). Acting as a protective colloid, its structure of polysaccharides and proteins formed a network that hinders particle aggregation, thus ensuring the chromatic and protein stability of the product ((tenutalamacchia.,) "https://www.tenutalamacchia.com/la-gomma-nel-vino-come-elemento-di-stabilita-e-non-solo/, Access on 18-12-2025" n. d.). Consequently, the application of aqueous Arabic gum solutions has become a consolidated practice in the industry, particularly during the refinement and stabilization stage of red and sparkling wines (Apolinar-Valiente et al., 2020b; Nigen et al., 2019b). However, during the operations of clarification, filtration, and plant cleaning, a significant fraction of such solutions was inevitably discarded in the form of wastewater containing Arabic gum in diluted concentration ((tenutalamacchia.,)"https://www.tenutalamacchia.com/la-gomma-nel-vino-come-elemento-di-stabilita-e-non-solo/, Access on 18-12-2025" n. d.).

A feasibility study based on Italian production volumes recorded in 2024 allowed estimating the applicability of the recycled Arabic gum within the steel supply chain. Analyzing the supply side, against a national wine production equal to 44.1×10^6 hL ((oiv.int,) "https://www.oiv.int/it/what-we-do/country-report?oiv, access on 26-02-26" n. d.), a theoretical consumption of about 1323 tons of raw Arabic gum was estimated (Nigen et al., 2019b). Assuming that 80-90 wt% of the raw material was contained in the equivalent waste, the actual availability of recycled Arabic gum stood at about 1055-1192 tons. Considering that the Italian annual mill scale production was approximately 400,000 tons (the 2% of steel produced) ((eurofer.,) "https://www.eurofer.eu/publications/brochures-booklets-and-factsheets/european-steel-in-figures-2025, access on 18-02-2026" n. d.; (ispatguru.,) "https://www.ispatguru.com/mill-scale/, access on 20-03-26" n. d.), the recycled Arabic gum was only able to cover up to 4% of the demand to produce the briquettes tested in this work, according to the different mixture (Fig. 13).

However, it is important to underline that such results, although indicating the impossibility of a total substitution of starch on a global scale, presented a margin for improvement, especially considering that the calculation was based on the conservative hypothesis in which all the mill scale produced is destined for the production of self-reducing briquettes, thus excluding other valorization or industrial reuse route (Nowacki et al., 2021). Approximately, the 90% of mill scale is indeed directly recycled in steelmaking industry or used in ferroalloys production, in cement plant or petrochemical industry (Alghtani et al., 2022; Iluțiu - Varvara et al., 2020). Consequently, considering only the 10% of scale still not valorized, the recycled Arabic gum would cover up to 46% of the demand, according to the selected mixture.

4. Conclusion

The feasibility of replacing corn starch as a binder with a recycled Arabic gum solution was evaluated through a comparison of the mechanical and metallurgical properties of self-reducing briquettes made of mill scale and three different reducing agents (two olive pomaces pyrolyzed at 750 (OP750) and 350 °C (OP350), and a cupola furnace dust (CFD)). The main results are summarized as follows:

- The optimal water-solid ratio identified in the recycled Arabic gum is 1.88:1. A reduced amount of water causes dryness and easier breakage of the agglomerate, while an excessive amount was released without improving the briquette's performance.
- Starch only favored higher densification in systems containing coarse particles such as olive pomaces, increasing the cured density by 17-21%. However, recycled Arabic gum increased the IRI of all the mixtures, raising it to 1000 with the OP750 and CFD, and increasing it by 278% with the OP350. Conversely, the Arabic gum reduced the UCS of OP750 by 46%.
- Corn starch acted as a viscous gel and arranged the mill scale orthogonally to the briquetting direction increasing the compression resistance of OP750. Recycled Arabic gum, being more fluid, instead favored the alignment of mill scale particles parallel to the load axis, resulting in a more homogeneous distribution and reduced mechanical resistance.
- Briquettes agglomerated with starch underwent to catastrophic swelling of over 20% with OP750 and OP350, while recycled Arabic gum favored advantages in thermal stability the shrinkage in all the mixtures tested, with values of approximately −40% for mixtures with olive pomace and −32% for the mixture with CFD at 1200 °C.
- Although the chemical composition, the microstructure of the metallic phase, and of the mineralogy of the slag remained unchanged according to the binder used, the degree of metallization with OP350 and CFD mixtures increased by 9 and 2% using recycled Arabic gum. On the contrary, the latter limited the complete smelting with OP750, with some slag remaining attached to the metallic matrix.

CRediT authorship contribution statement

Sara Scolari: Writing – original draft, Validation, Resources, Methodology, Investigation, Formal analysis, Data curation, Conceptualization. **Luca Tosarello:** Writing – review & editing, Validation, Methodology, Investigation. **Davide Mombelli:** Writing – review & editing, Validation, Methodology, Conceptualization. **Gianluca Dall'Osto:** Writing – review & editing. **Carlo Mapelli:** Supervision.

Funding

The work was funded by European Union - NextGenerationEU, Mission 4, Component 2, Investment 1.1, PRIN 2022 project -"Low environmental impact fuels for metallurgical industries", CUP D53D23003860006, Prot. 2022P3PJXN.

Declaration of competing interest

The authors declare that they have no known competing financial interests or personal relationships that could have appeared to influence the work reported in this paper.

Acknowledgements

The authors would like to acknowledge AEB S. p.A., in particular, Dr. Matteo Este and Dr. Paolo Machiavelli, for supplying the recycled solution of Arabic gum.

Appendix A. Supplementary data

Supplementary data to this article can be found online at https://doi.org/10.1016/j.partic.2026.06.039.

References

Abdelrahim, A., Aula, M., Iljana, M., Willms, T., Echterhof, T., Steinlechner, S., et al. (2021). Suitability of self-reducing and slag-forming briquettes for electric Arc furnace use based on laboratory tests. *Steel Research International, 93*(2). https://doi.org/10.1002/srin.202100472

Abdelrahim, A., Aula, M., Iljana, M., Willms, T., Echterhof, T., Steinlechner, S., et al. (2022). Suitability of self-reducing and slag-forming briquettes for electric Arc furnace use based on laboratory tests. *Steel Research International, 93*(2). https://doi.org/10.1002/srin.202100472

Adu-Poku, K. A., Appiah, D., Asosega, K. A., Derkyi, N. S. A., Uba, F., Kumi, E. N., et al. (2022). Characterization of fuel and mechanical properties of charred agricultural wastes: Experimental and statistical studies. *Energy Reports, 8*, 4319–4331. https://doi.org/10.1016/j.egyr.2022.03.015

Alghtani, A. H., Alsharef, M., & El-Aziz, K. A. (2022). Characterization of iron powder produced by reduction of hot-rolled mill scale in hydrogen gas. *Materials Research, 25*. https://doi.org/10.1590/1980-5373-mr-2021-0575

Andersson, A., Gullberg, A., Kullerstedt, A., Ahmed, H., Sundqvist-Ökvist, L., & Samuelsson, C. (2019). Upgrading of blast furnace sludge and recycling of the low-zinc fraction via cold-bonded briquettes. *Journal of Sustainable Metallurgy, 5*(3), 350–361. https://doi.org/10.1007/s40831-019-00225-x

Apolinar-Valiente, R., Salmon, T., Williams, P., Nigen, M., Sanchez, C., Marchal, R., & Doco, T. (2020a). Improvement of the foamability of sparkling base wines by the addition of Acacia gums. *Food Chemistry, 313*, Article 126062. https://doi.org/10.1016/j.foodchem.2019.126062

Apolinar-Valiente, R., Salmon, T., Williams, P., Nigen, M., Sanchez, C., Marchal, R., & Doco, T. (2020b). Improvement of the foamability of sparkling base wines by the addition of Acacia gums. *Food Chemistry, 313*, Article 126062. https://doi.org/10.1016/j.foodchem.2019.126062

Bagatini, M. C., Fernandes, T., Silva, R., Galvão, D. F., & Flores, I. V. (2020). Mill scale and flue dust briquettes as alternative burden to low height blast furnaces. *Journal of Cleaner Production, 276*. https://doi.org/10.1016/j.jclepro.2020.124332

Bagatini, M. C., Zymla, V., Osório, E., & Vilela, A. C. F. (2017). Scale recycling through self-reducing briquettes to use in EAF. *ISIJ International, 57*(12), 2081–2090. https://doi.org/10.2355/isijinternational.ISIJINT-2017-242

Barisetty, S., Kalshetty, S., Ramakrishna, S., Vishwanath, S. C., & Balachandran, G. (2020). Cold briquetting of DRI fines for use in steel making process. *Transactions of the Indian Institute of Metals, 73*(2), 449–455. https://doi.org/10.1007/s12666-019-01856-0

bayrony https://bayrony.com/product-enquiry/products/gum-arabic/. ((n.d.)).

Blesa, M. J., Miranda, J. L., Izquierdo, M. T., & Moliner, R. (2003). Curing time effect on mechanical strength of smokeless fuel briquettes. *Fuel Processing Technology, 80*, 155–167.

Borowski, G., Stępniewski, W., & Wójcik-Oliveira, K. (2017). Effect of starch binder on charcoal briquette properties. *International Agrophysics, 31*(4), 571–574. https://doi.org/10.1515/intag-2016-0077

Carotenuto, G. (2023). Particle-settling in iper-viscous liquids and its use for time measurement. *Materials Science*, 1–5.

Chen, W.-H., Peng, J., & Bi, X. T. (2015). A state-of-the-art review of biomass torrefaction, densification and applications. *Renewable and Sustainable Energy Reviews, 44*, 847–866. https://doi.org/10.1016/j.rser.2014.12.039

Cui, K. F. E., Zhou, G. G. D., & Jing, L. (2021). Viscous effects on the particle size segregation in geophysical mass flows: Insights from immersed granular shear flow simulations. *Journal of Geophysical Research: Solid Earth, 126*(8). https://doi.org/10.1029/2021JB022274

Dall'Osto, G., Gondorf, C., Firoozbakht, M., Mombelli, D., Commer, M., Mapelli, C., & Wuppermann, C. (2026). Promoting circular economy in cast Iron production through Co-charging of mill scale–biochar agglomerates and scrap in an induction furnace. *International Journal of Metalcasting*. https://doi.org/10.1007/s40962-026-01945-z

Dall'Osto, G., Mombelli, D., Pittalis, A., & Mapelli, C. (2023). Biochar and other carbonaceous materials used in steelmaking: Possibilities and synergies for power generation by direct carbon fuel cell. *Biomass and Bioenergy, 177*, Article 106930. https://doi.org/10.1016/j.biombioe.2023.106930

Dall'Osto, G., Mombelli, D., Scolari, S., & Mapelli, C. (2024). Role of the biogenic carbon physicochemical properties in the manufacturing and industrial transferability of mill scale-based self-reducing briquettes. *Metals, 14*(8), 882. https://doi.org/10.3390/met14080882

Dall'Osto, G., Mombelli, D., Trombetta, V., & Mapelli, C. (2024). Effect of particle size and starch gelatinization on the mechanical and metallurgical performance of jarosite plus blast furnace sludge self-reducing briquettes. *Journal of Sustainable Metallurgy*. https://doi.org/10.1007/s40831-024-00825-2

Dall'Osto, G., Scolari, S., Mombelli, D., & Mapelli, C. (2025). Survey on the valorization of wood and agribusiness wastes for their application as fossil carbon substitutes in metallurgical processes. *Biomass Conversion and Biorefinery*. https://doi.org/10.1007/s13399-025-06707-1

De Melo Silva Cheloni, L. M., da Veiga Lopes, L. A., & Reis, E. L. (2024). Compressive strength behavior of briquettes produced from manganese ore fines and metal dust: Optimization using response surface methodology. *Mineral Processing and Extractive*

Metallurgy Review, 45(6), 592–605. https://doi.org/10.1080/08827508.2023.2212115
Ding, Y., & Yue, Z. Q. (2018). An experimental investigation of the roles of water content and gas decompression rate for outburst in coal briquettes. *Fuel, 234*, 1221–1228. https://doi.org/10.1016/j.fuel.2018.07.143
Drobíková, K., Plachá, D., Motyka, O., Gabor, R., Kutláková, K. M., Vallová, S., & Seidlerová, J. (2016). Recycling of blast furnace sludge by briquetting with starch binder: Waste gas from thermal treatment utilizable as a fuel. *Waste Management, 48*, 471–477. https://doi.org/10.1016/j.wasman.2015.11.047
Echterhof, T., Willms, T., Preiß, S., Omran, M., Fabritius, T., Mombelli, D., et al. (2019). Tecnologie pulite per la produzione d'acciaio Developing a new process to agglomerate secondary raw material fines for recycling in the electric arc furnace-the fines2EAF project. *La Metallurgia Italiana-n, 5*, 31–40.
Elsadek, M., Mousa, E., & Ahmed, H. (2024). Green approach to ironmaking: Briquetting and hydrogen reduction of mill scale using novel binders. *International Journal of Hydrogen Energy, 62*, 732–738. https://doi.org/10.1016/j.ijhydene.2024.03.152
Emami, S., & Tabil, L. G. (2008). Friction and compression characteristics of chickpea flour and components. *Powder Technology, 182*(1), 119–126. https://doi.org/10.1016/j.powtec.2007.07.012
enartis. https://www.enartis.com/wp-content/uploads/2021/05/Enartis-Newsletter-ArabicGum-EN-SA.pdf, access on 18-December-2026. ((n.d.)).
eurofer. https://www.eurofer.eu/publications/brochures-booklets-and-factsheets/european-steel-in-figures-2025, access on 18-February-2026. ((n.d.)).
Ezeakacha, C. P., Rabbani, A., Salehi, S., & Ghalambor, A. (2018). Integrated image processing and computational techniques to characterize formation damage. In *SPE international conference and exhibition on formation damage control*. SPE. https://doi.org/10.2118/189509-MS.
Fanfoni, M., & Tomellini, M. (1998). The Johnson-Mehl- Avrami-Kohnogorov model: A brief review. *Il Nuovo Cimento - B D, 20*(7–8), 1171–1182. https://doi.org/10.1007/BF03185527
Fine, R. A., & Millero, F. J. (1973). Compressibility of water as a function of temperature and pressure. *The Journal of Chemical Physics, 59*(10), 5529–5536. https://doi.org/10.1063/1.1679903
García, F. A., Campoy, P., Mochón, J., Ruiz-Bustinza, I., Verdeja, L. F., & Duarte, R. M. (2010). A new "User-friendly" blast furnace advisory control system using a neural network temperature profile classifier. *ISIJ International, 50*(5), 730–737. https://doi.org/10.2355/isijinternational.50.730
horiba. https://www.horiba.com/int/scientific/products/particle-characterization/particle-education/setting-particle-size-specifications/. ((n.d.)).
Idirs, O. H. M. (2017). What is gum Arabic? An overview. *Int. J. Sudan Research, 7*(1), 1–14.
Ilutiu-Varvara, D.-A., Tintelecan, M., Aciu, C., & Sas-Boca, I.-M. (2020). *Reuse of the steel mill scale for sustainable industrial applications* (p. 14). Basel Switzerland: MDPI: The 14th International Conference on Interdisciplinarity in Engineering—INTER-ENG. https://doi.org/10.3390/proceedings2020063014, 2020.
Iluțiu - Varvara, D.-A., Aciu, C., Tintelecan, M., & Sas - Boca, I.-M. (2020). Assessment of recycling potential of the steel mill scale in the composition of mortars for sustainable manufacturing. *Procedia Manufacturing, 46*, 131–135. https://doi.org/10.1016/j.promfg.2020.03.020
ispatguru. https://www.ispatguru.com/mill-scale/, access on 20-March-26. ((n.d.)).
Jin, N., Kong, D., & Wang, H. (2019). Effects of temperature and time on gelatinization of corn starch employing gradient isothermal heating program of rapid visco analyzer. *Journal of Food Process Engineering, 42*(7). https://doi.org/10.1111/jfpe.13264
Kabakcı, S. B., & Aydemir, H. (2014). Pyrolysis of olive pomace and copyrolysis of olive pomace with refuse derived fuel. *Environmental Progress & Sustainable Energy, 33*(2), 649–656. https://doi.org/10.1002/ep.11827
Koohestani, H., Hasanpoor, J., & Ghasemi, B. (2025). Eco-friendly steelmaking: Exploring the potential of plant-based binder acacia gum for iron ore pelletizing. *Case Studies in Chemical and Environmental Engineering, 11*, Article 101110. https://doi.org/10.1016/j.cscee.2025.101110
Kumar, D. S., Sah, R., Sekhar, V. R., & Vishwanath, S. C. (2017). Development and use of mill scale briquettes in BOF. *Ironmaking and Steelmaking, 44*(2), 134–139. https://doi.org/10.1080/03019233.2016.1165499
Leino, T., Taskinen, P., & Eric, R. H. (2020). Determination of metallization degree of pre-reduced chromite with image and rietveld analysis. *Journal of Mining and Metallurgy, Section B: Metallurgy, 56*(3), 289–297. https://doi.org/10.2298/JMMB200313022L
Liu, G., Lian, L., & Liu, Y. (2024). Carbothermal reduction assisted by hydrogenation treatment for preparing single-phase CeC_2 nanoscale powders. *Materials Research Express, 11*(1), Article 015601. https://doi.org/10.1088/2053-1591/ad1075
Lohmeier, L., Thaler, C., Harris, C., Wollenberg, R., & Schröder, H.-W. (2020). Briquetting of fine-grained residues from iron and steel production using organic and inorganic binders. *Steel Research International, 91*(12). https://doi.org/10.1002/srin.202000238
Lustosa Filho, J. F., da Silva, A. P. F., Costa, S. T., Gomes, H. T., de Figueiredo, T., & Hernández, Z. (2024). Biochars derived from olive mill byproducts: Typology, characterization, and eco-efficient application in agriculture—A systematic review. *Sustainability, 16*(12), 5004. https://doi.org/10.3390/su16125004
Mantovani, M. C., & Cyro, T. (2000). The strength and the high temperature behaviors of self-reducing pellets containing EAF dust. *ISIJ International, 40*, 224–230.
Mantovani, M. C., Takano, C., & Büchler, P. M. (2002). Electric arc furnace dust-coal composite pellet: Effects of pellet size, dust composition, and additives on swelling and zinc removal. *Ironmaking and Steelmaking, 29*(4), 257–265. https://doi.org/10.1179/030192302225004494
Mombelli, D., Di Cecca, C., Mapelli, C., Barella, S., & Bondi, E. (2016). Experimental analysis on the use of BF-sludge for the reduction of BOF-Powders to direct reduced iron (DRI) production. *Process Safety and Environmental Protection, 102*, 410–420. https://doi.org/10.1016/j.psep.2016.04.017
Mombelli, D., Gonçalves, D. L., Mapelli, C., Barella, S., & Gruttadauria, A. (2021). Processing and characterization of self-reducing briquettes made of jarosite and blast furnace sludges. *Journal of Sustainable Metallurgy, 7*(4), 1603–1626. https://doi.org/10.1007/s40831-021-00419-2
Mombelli, D., Mapelli, C., Barella, S., Gruttadauria, A., & Spada, E. (2019). Jarosite wastes reduction through blast furnace sludges for cast iron production. *Journal of Environmental Chemical Engineering, 7*(2). https://doi.org/10.1016/j.jece.2019.102966
Mousa, E., Ahmed, H., & Söderström, D. (2022). Potential of alternative organic binders in briquetting and enhancing residue recycling in the steel industry. *Recycling, 7*(2), 21. https://doi.org/10.3390/recycling7020021
Müller, N., Herz, G., Reichelt, E., Jahn, M., & Michaelis, A. (2021). Assessment of fossil-free steelmaking based on direct reduction applying high-temperature electrolysis. *Cleaner Engineering and Technology, 4*, Article 100158. https://doi.org/10.1016/j.clet.2021.100158
Nath, S. K., Rajshekar, Y., Alex, T. C., Venugopalan, T., & Kumar, S. (2017). Evaluation of the suitability of alternative binder to replace OPC for iron ore slime briquetting. *Transactions of the Indian Institute of Metals, 70*(8), 2165–2174. https://doi.org/10.1007/s12666-017-1038-5
Nigen, M., Valiente, R. A., Iturmendi, N., Williams, P., Doco, T., Moine, V., et al. (2019a). The colloidal stabilization of young red wine by Acacia Senegal gum: The involvement of the protein backbone from the protein-rich arabinogalactan-proteins. *Food Hydrocolloids, 97*, Article 105176. https://doi.org/10.1016/j.foodhyd.2019.105176
Nigen, M., Valiente, R. A., Iturmendi, N., Williams, P., Doco, T., Moine, V., et al. (2019b). The colloidal stabilization of young red wine by Acacia Senegal gum: The involvement of the protein backbone from the protein-rich arabinogalactan-proteins. *Food Hydrocolloids, 97*, Article 105176. https://doi.org/10.1016/j.foodhyd.2019.105176
Ning, X., Ren, Z., Zhang, N., Wang, G., Zhang, X., Wu, J., et al. (2025). Reduction study of carbon-bearing briquettes in the system of multiple reductants. *Materials, 18*(18), 4408. https://doi.org/10.3390/ma18184408
Nowacki, K., Maciąg, T., & Lis, T. (2021). Recovery of iron from mill scale by reduction with carbon monoxide. *Minerals, 11*(5), 529. https://doi.org/10.3390/min11050529
oiv.int https://www.oiv.int/it/what-we-do/country-report?oiv, access on 26-February-26. ((n.d.)).
Okegbile, O., Baba Hassan, A., Okegbile, O. J., Hassan, A. B., Mohammed, A., & Irekeola, B. J. (2014). Effect of starch and gum Arabic binders in the combustion characteristics of briquette prepared from sawdust. *Article in International Journal of Scientific and Engineering Research, 5*(3). http://www.ijser.org.
Olugbade, T., Ojo, O., & Mohammed, T. (2019). *Influence of binders on combustion properties of biomass briquettes: A recent review*. New York: *Bioenergy Research*. Springer. https://doi.org/10.1007/s12155-019-09973-w. LLC.
Pang, L., Yang, Y., Wu, L., Wang, F., & Meng, H. (2019). Effect of particle sizes on the physical and mechanical properties of briquettes. *Energies, 12*(19). https://doi.org/10.3390/en12193618
Patil, D. P., Taulbee, D., Parekh, B. K., & Honaker, R. (2009). Briquetting of coal fines and sawdust - Effect of particle-size distribution. *International Journal of Coal Preparation and Utilization, 29*(5), 251–264. https://doi.org/10.1080/19392690903294423
Pauluzzi, D., & Martinis, A. (2018). *Sustainable decrease OF CO2 emissions in the steelmaking industry by means of the ENERGIRON direct reduction technology*.
Quddus, M., Rahman, M., Khanam, J., Biswas, B., Sharmin, N., Ahmed, S., & Neger, A. (2018). Synthesis and characterization of pigment grade red iron oxide from mill scale. *International Research Journal of Pure and Applied Chemistry, 16*(4), 1–9. https://doi.org/10.9734/IRJPAC/2018/42935
Rabbani, A., & Salehi, S. (2017). Dynamic modeling of the formation damage and mud cake deposition using filtration theories coupled with SEM image processing. *Journal of Natural Gas Science and Engineering, 42*, 157–168. https://doi.org/10.1016/j.jngse.2017.02.047
Raveendran, K., & Ganesh, A. (1996). Heating value of biomass and biomass pyrolysis products. *Fuel, 75*(15), 1715–1720. https://doi.org/10.1016/S0016-2361(96)00158-5
Richards, S. (1990). Briquetting peat and peat-coal mixtures. *Fuel Processing Technology, 25*(3), 175–190.
Sachdev, D., Gupta, S., Bhullar, N. K., & Verma, G. (2025). Recent progress on the correlation between hydrophobicity and the water absorption of different materials. *Journal of Inorganic and Organometallic Polymers and Materials, 35*(7), 5261–5286. https://doi.org/10.1007/s10904-024-03586-3
Salimbeni, A., Lombardi, G., Rizzo, A. M., & Chiaramonti, D. (2023). Techno-economic feasibility of integrating biomass slow pyrolysis in an EAF steelmaking site: A case study. *Applied Energy, 339*, Article 120991. https://doi.org/10.1016/j.apenergy.2023.120991
Sanchez, C., Nigen, M., Mejia Tamayo, V., Doco, T., Williams, P., Amine, C., & Renard, D. (2018). Acacia gum: History of the future. *Food Hydrocolloids, 78*, 140–160. https://doi.org/10.1016/j.foodhyd.2017.04.008
Scolari, S., Dall'Osto, G., Tuveri, A., Mombelli, D., & Mapelli, C. (2025). Optimization of red mud and blast furnace sludge self-reducing briquettes propaedeutic for subsequent magnetic separation. *Metals, 15*(10), 1108. https://doi.org/10.3390/met15101108
Scolari, S., Mombelli, D., Dall'Osto, G., & Mapelli, C. (2025). Effect of water-powder interaction on the mechanical and metallurgical behavior of integrated steel plant byproducts agglomerates. *Particuology, 105*, 74–87. https://doi.org/10.1016/j.partic.2025.07.019

Scolari, S., Mombelli, D., Dall'Osto, G., & Mapelli, C. (2026). Feasibility study on use of Arabic gum as alternative to corn starch in bonding self-reducing briquettes made by integrated cycle by-products. *Particuology, 110*, 96–108. https://doi.org/10.1016/j.partic.2026.01.008

Sen, R., Wiwatpanyaporn, S., & Annachhatre, A. P. (2016). Influence of binders on physical properties of fuel briquettes produced from cassava rhizome waste. *International Journal of Environment and Waste Management, 17*.

Singh, M., & Bjorkman, B. (2004). Effect of reduction conditions on the swelling behaviour of cement-bonded briquettes. *ISIJ International, 44*(2), 294–303.

Singh, M., & Bjorkman, B. (2004). Effect of processing parameters on the swelling behaviour of cement-bonded briquettes. *ISIJ International, 44*(1), 59–68.

Somerville, M. A. (2016). The strength and density of green and reduced briquettes made with iron ore and charcoal. *Journal of Sustainable Metallurgy, 2*(3), 228–238. https://doi.org/10.1007/s40831-016-0057-5

Sotannde, O. A., Oluyege, A. O., & Abah, G. B. (2009). Physical and combustion properties of charcoal briquettes from neem wood residues. *International Agrophysics, 24*, 189–194.

Sotannde, O. A., Oluyege, A. O., & Abah, G. B. (2010). Physical and combustion properties of briquettes from sawdust of Azadirachta indica. *Journal of Forestry Research, 21*(1), 63–67. https://doi.org/10.1007/s11676-010-0010-6

Takano, C., & Mourao, M. B. (2003). Self-reducing pellets for ironmaking: Mechanical behavior. *Mineral Processing and Extractive Metallurgy Review, 24*(3–4), 233–252. https://doi.org/10.1080/714856823

tenutalamacchia. https://www.tenutalamacchia.com/la-gomma-nel-vino-come-elemento-di-stabilita-e-non-solo/, Access on 18-December-2025. ((n.d.)).

tridge. https://www.tridge.com/, access on 15/December/25. ((n.d.)).

Trpčevská, J., Piroskova, J., & Pribulova, A.. Alternative binding materials for the briquettes production from the metallurgical wastes hard zinc processing, production of alloys from zinc drosses view project. https://www.researchgate.net/publication/282307792. n.d.

Tumuluru, J. S., & Wright, C. T (2010). A review on biomass densification technologie for energy application. https://doi.org/10.2172/1016196.

Valenti, F., Arcidiacono, C., Chinnici, G., Cascone, G., & Porto, S. M. (2017). Quantification of olive pomace availability for biogas production by using a GIS-based model. *Biofuels, Bioproducts and Biorefining, 11*(5), 784–797. https://doi.org/10.1002/bbb.1784

Wei, R., Cang, D., Bai, Y., Huang, D., & Liu, X. (2016). Reduction characteristics and kinetics of iron oxide by carbon in biomass. *Ironmaking and Steelmaking, 43*(2), 144–152. https://doi.org/10.1179/1743281215Y.0000000061

Wu, J., Wu, S., An, G., Ma, C., Teng, Z., Xu, K., et al. (2023). Study on direct reduction in carbon-bearing pellets using biochar. *Sustainability, 15*(24), Article 16554. https://doi.org/10.3390/su152416554

Yahaya, D. B., & Ibrahim, T. G. (2012). Development of rice husk briquettes for use as fuel. *Research Journal in Engineering and Applied Sciences, 1*(2), 130–133. www.emergingresource.org.

Yu, W., Sun, T., Liu, Z., Kou, J., & Xu, C. (2014). Effects of particle sizes of iron ore and coal on the strength and reduction of high phosphorus oolitic hematite-coal composite briquettes. *ISIJ International, 54*(1), 56–62. https://doi.org/10.2355/isijinternational.54.56

Zepeda-Cepeda, C. O., Goche-Télles, J. R., Palacios-Mendoza, C., Moreno-Anguiano, O., Núñez-Retana, V. D., Heya, M. N., & Carrillo-Parra, A. (2021). Effect of sawdust particle size on physical, mechanical, and energetic properties of Pinus durangensis briquettes. *Applied Sciences, 11*(9), 3805. https://doi.org/10.3390/app11093805

Zhu, Y., Wei, Y., Fan, W., Chareyre, B., Wu, C., & Kido, R. (2025). Numerical investigation on effects of particle size distribution on loess mechanics using DEM. *Environmental Earth Sciences, 84*(21), 618. https://doi.org/10.1007/s12665-025-12642-1